General Disclaimer

One or more of the Following Statements may affect this Document

- This document has been reproduced from the best copy furnished by the organizational source. It is being released in the interest of making available as much information as possible.

- This document may contain data, which exceeds the sheet parameters. It was furnished in this condition by the organizational source and is the best copy available.

- This document may contain tone-on-tone or color graphs, charts and/or pictures, which have been reproduced in black and white.

- This document is paginated as submitted by the original source.

- Portions of this document are not fully legible due to the historical nature of some of the material. However, it is the best reproduction available from the original submission.

NATIONAL AERONAUTICS AND SPACE ADMINISTRATION

Technical Memorandum 33-423

Mariner Venus 67 Power Subsystem Modification: Test and Flight Operation

A. Krug

NI

JET PROPULSION LABORATORY
CALIFORNIA INSTITUTE OF TECHNOLOGY
PASADENA, CALIFORNIA

June 30, 1969

NATIONAL AERONAUTICS AND SPACE ADMINISTRATION

Technical Memorandum 33-423

Mariner Venus 67 Power Subsystem Modification: Test and Flight Operation

A. Krug

JET PROPULSION LABORATORY
CALIFORNIA INSTITUTE OF TECHNOLOGY
PASADENA, CALIFORNIA

June 30, 1969

Prepared Under Contract No. NAS 7-100
National Aeronautics and Space Administration

Preface

The work described in this report was performed by the Guidance and Control Division of the Jet Propulsion Laboratory.

Acknowledgment

The author wishes to acknowledge the contributions of numerous Jet Propulsion Laboratory personnel who assisted in the *Mariner* Venus 67 power subsystem effort. In particular, J. V. Goldsmith, W. K. Shubert, and S. Krause contributed their expertise in the design and fabrication of the solar panels, power conditioning equipment, and the battery, respectively, as well as much of the material contained in this technical memorandum.

Contents

I. Introduction 1

II. Power Subsystem 1

A. Solar Panel 1

1. Design 1

2. Testing 2

B. Power Conditioning 2

1. Design 2

2. Testing 3

C. Battery 4

1. Design 4

2. Testing 4

D. Power System Flight Operation 5

III. Solar Panel Design and Test 5

A. Solar Panel Substrate Design 6

B. Zener Diode Shunt Regulator 7

C. Solar Cell Assembly 7

D. Solar Cell Submodule 11

E. Solar Panel Submodule Manufacturing 11

F. Solar Array Temperature Monitoring 11

G. I_{sc}–V_{oc} Transducer 12

H. Solar Array Assembly 13

I. Environmental Qualification Testing 13

J. Predicted Array Thermal Characteristics 13

K. Electrical Performance Testing 14

L. Electrical Performance Characteristics 16

M. Solar Panel Flight Operation 16

IV. Conditioning Equipment Modification and Test 19

A. *Mariner* Mars 1964 Configuration 19

1. Case I power distribution module (4A11) 21

2. Case I power synchronizer (4A12) 21

3. Case I battery charger (4A13) 21

4. Case I main 2.4 kHz inverter (4A15) 21

Contents (contd)

5. Case I maneuver 2.4 kHz inverter (4A16) 21

6. Case I 400-Hz single phase inverter (4A17) 21

7. Case I 400-Hz three phase inverter (4A18) 21

B. Changes from *Mariner* Mars 1964 PCE due to Changed Power Requirements 21

C. Command Logic Changes from *Mariner* Mars 1964 PCE 22

D. Battery Voltage Telemetry Circuit 22

E. *Mariner* Venus 67 PCE Configuration 22

F. Detail Design Changes to the *Mariner* Mars 1964 PCE 22

G. Design Changes Required Because of *Mariner* Venus 67 Systems Testing 23

1. Difficulty with 4A8 50-MHz RFI 23

2. Battery charger false switching 25

H. Environmental Testing 25

I. Time Scale for Modifications 26

J. PCE Performance During Launch and Midcourse Maneuver 26

V. Battery Modification and Test 26

A. Design Changes 27

1. Potting cover 27

2. Negative plate 27

3. Cellophane separator 27

B. Construction Details 27

C. Discussion 27

1. Design and construction 27

2. Test program 28

3. Flight acceptance requirements 29

D. Conclusions 30

E. Battery Flight Operation 32

Tables

1. Solar panel description 5

2. *Mariner* Venus 67 solar panel; data reduced to 135 mW/cm² and 58°C . . . 15

3. Power conditioning inputs and outputs 21

Contents (contd)

Tables (contd)

4. B/R power leads 22
5. Commands and controls 23
6. Comparison of batteries 28
7. Battery discharge comparisons 30

Figures

1. *Mariner* Venus 67 solar panel 6
2. Schematic of typical electrical station 7
3. Solar panel, rear surface 7
4. Solar panel, front surface 8
5. Closeup of I_{sc}–V_{oc} transducer 9
6. Closeup of typical temperature transducer installation 9
7. Average individual solar cell current-voltage curves for *Mariner* Venus 67 9
8. Typical solar cell submodule: (a) front, (b) rear 10
9. Submodule tunnel oven 11
10. Cell emplacement in the solder boat 11
11. Assembled cells and N contact bus bar in a submodule boat 12
12. Assembling the submodule solder boat 12
13. Predicted solar panel temperature during Venus mission 14
14. Predicted *Mariner* Venus 67 solar panel temperature vs solar intensity 14
15. Solar panel temperature rise induced by Venus 15
16. Midcourse maneuver temperature history for *Mariner* Venus 67 15
17. General equations used in determining the intensity-voltage characteristics of a *Mariner* Venus 67 solar panel 15
18. Absolute space power capability contingencies prediction capability for a panel in space at some heliocentric distance based on Table Mountain predictions 16
19. Total undegraded spacecraft solar panel peak raw power vs heliocentric distance 17
20. Variation of panel section performance with intensity; for array characteristics the power is multiplied by 12 17
21. Total panel power vs voltage for various conditions 17
22. Raw data curve for *Mariner* Venus 67 solar panels: solar panel intensity-voltage curve 17

Contents (contd)

Figures (contd)

23. Solar array reduced data for *Mariner* Venus 67 voltage-intensity curve 18
24. Solar panel substrate temperature vs mission time 18
25. Solar panel spar-zener temperature vs mission time 18
26. Mission time vs I_{sc} cell output 18
27. Mission time vs I_{sc_T} cell output 19
28. Mission time vs V_{oc} cell output 19
29. Power subsystem mechanization for *Mariner* Mars 1964 20
30. *Mariner* Venus 67 power subsystem 24
31. Diode reverse recovery characteristics 25
32. Battery charger switching circuit 25
33. PS&L voltage 27
34. Total solar panel current 27
35. Test procedure flow diagram 29
36. Cell voltages at 32°F ambient temperature, 5-A load cutoff point, and 26.29-V terminal voltage 29
37. Discharge curve for battery 26 at 32°F ambient temperature and 5-A discharge rate 30
38. Discharge curve at 140°F ambient temperature and 10-A discharge rate . . . 30
39. Battery terminal voltage profile; launch to second Canopus acquisition . . . 32
40. Battery charger current profile; launch to second Canopus acquisition 32
41. Battery terminal voltage; launch to end of mission 33

Abstract

Spare spacecraft originally designed for the *Mariner* Mars 1964 mission were modified to accomplish the successful Venus flyby of *Mariner V*. This technical memorandum describes the changes necessary to the power subsystem of that spacecraft to adapt it for the Venus mission.

Flying toward rather than away from the sun affected the design of the primary power source—the solar panels. The panels were required to accommodate temperatures in excess of 120°C, and to supply power within a voltage range compatible with the power conditioning equipment. Thermal interactions between the solar panels and the spacecraft mechanical bus also affected the design.

The power conditioning equipment design was affected by the scientific instrument package which was flown, and the entirely new sequence of operations at planet encounter. The power conditioning equipment was redesigned, therefore, to provide the increased power handling capability required by the spacecraft loads, and the revised switching of the power distributed to the scientific instrument package.

The battery design remained slightly redesigned for *Mariner* Venus 67; however, new batteries were fabricated for the mission.

The test, operations, and flight of the *Mariner* Venus 67 power subsystem were extremely successful; a minimum of difficulties were encountered.

Mariner Venus 67 Power Subsystem Modification: Test and Flight Operation

I. Introduction

The *Mariner* Mars 1964 spare power conditioning units and newly fabricated solar panels and batteries provided the flight and flight spare spacecraft units for the power subsystem for *Mariner* Venus 67. The fact that the spacecraft was to fly toward rather than away from the sun caused the redesign and fabrication of new solar panels. The batteries were slightly redesigned to provide some improvements since new batteries would be required for the flight and flight spares. The *Mariner* Mars 1964 batteries were 2–3 yr old from activation and were not considered reliable for flight at that age. The power conditioning required modification and the fabrication of new main 2.4 kHz inverters because of increased power requirements and revised load switching sequences.

II. Power Subsystem

A. Solar Panel

1. Design. The change in direction from a Mars to a Venus mission had its greatest effect on the solar panels of the power subsystem. On the Mars mission, with the spacecraft moving away from the sun, the solar intensity and, consequently, the temperature decreased with time. Under such conditions, a characteristic of the solar cell was a decreasing power output with increasing voltage. Conversely, on the Venus mission, the solar intensity and temperature increased with time; however, the voltage decreased. Therefore, the series-parallel arrangement of cells in each panel section had to be revised to provide more cells in series since the output voltage of the *Mariner C* panel (84 cells in series) would be only 30 V at Venus encounter. This low panel voltage would cause uncontrollable sharing between the panels and the battery.

Another consideration in the panel design was the panel mounting location. Because of the geometry of the earth–Venus mission, the spacecraft roll axis was reversed. The panels were also reversed and would have reflected heat from the celled surface into the electronic bays and vice versa, raising the temperatures above acceptable limits. This was relieved by eliminating 27 in. of substrate and solar cells next to the octagonal structure. The decision was made to leave the panels at the *Mariner* Mars 1964 length so as to use the attitude control gas systems without modification. This provided a total area of 43.6 ft^2 and a nominal power at launch of 400 W.

One problem in design was noted during space simulator testing of the type approval (TA) solar panel. The panel had been subjected to thermal shock tests of +130°F to −180°F and +165°F to −108°F with the appendages attached; e.g., attitude control gas systems, dual frequency receiver antennas, etc. In addition the panel had completed 48 h of the 60 h planned at +285°F when a facility power failure caused a loss of the solar simulator lights. The panel rapidly dropped in temperature from +285°F to −48°F. This shock caused numerous P-contact delaminations and a test program was immediately instituted to determine the extent of the problem. It was found that this shock rate represented an unrealistic test situation, and that inflight spacecraft could not turn rapidly enough, under normal circumstances, to cause a similar problem.

2. ***Testing.*** The spacecraft solar panels do not normally undergo the amount of system testing provided for other hardware. Two systems tests were performed using solar panels: the first test was the vibration of the flight spacecraft with the solar panels included. This test was designed to verify the tip-latched design. The second was a free mode test in which the solar panels were outside the Spacecraft Assembly Facility (SAF) building; the panels powered the spacecraft, which was located inside the SAF, by means of cables especially designed for this purpose. No problems were noted in either test. More specific information on solar panel testing is included in Section III.

B. Power Conditioning

1. Design. The changes required in the power conditioning equipment were mainly caused by the increased power demands of the new Data Automation System (DAS) and scientific instrument complement, and a design deficiency associated with the battery voltage monitor circuitry on *Mariner IV*. Because of the revised science instrument complement, the power distribution switching was also revised.

The *Mariner* Mars 1964 power subsystem main 2.4 kHz inverter was designed for a maximum continuous power load of 80 W and a peak load of 120 W. This inverter supplied power for all of the engineering loads (except the attitude/control (A/C) maneuver electronics, gyros and autopilot) and all of the science loads. With the science instruments and the new DAS, the total loading on this inverter was 90 to 105 W. To provide this output power within the nominal voltage regulation required a new output transformer; since the output transformer was potted into place it could not be removed without damage to the unit. Therefore, new main 2.4 kHz inverters were fabricated for this mission.

The revised power requirement created an additional problem in power handling capability. The *Mariner* Mars 1964 and *Mariner* Venus 67 power subsystems were designed to use the maneuver booster regulator (B/R) as a backup should the main B/R fail. The maneuver B/R is normally on only when the A/C gyros are required. However, if the main B/R should fail, this is sensed by the circuitry in the booster; the main spacecraft loads are then automatically switched onto the maneuver B/R. The capability of the main and maneuver boosters is 150 W, nominally. If a failure of the main B/R occurs and the gyros are required, the total load on the maneuver booster could be greater than 150 W. The main and maneuver boosters were integrated into one large case-size package that could not readily be modified to increase the power handling capability. To avoid this problem, an exclusive circuit was added to the B/R which would turn off science power in the event the main B/R failed and the gyros were on. Science power was not affected by either a main B/R failure or when only the gyros were on. A study of the problem of booster capability indicated that under certain conditions, discussed in Section IV, the booster could supply more than 150 W. Therefore, provision was made to override the exclusive circuit by ground command. The override was necessary for a critical condition, such as if the main booster fails and the gyros are required at Venus encounter.

One reason for the change in switching of the science instruments is their position on the *Mariner* Venus 67 spacecraft and the reversal of the spacecraft roll axis. These instruments, which were in the sun on the *Mariner* Mars 1964 mission, are on the shaded side of the spacecraft during the flight to Venus. Prior to launch, there was some concern about turning off the bus-mounted science instruments after encounter because they would become too cold and could not be returned to normal operation. The switching logic of the power distribution assembly for *Mariner* Mars 1964 allowed either the spacecraft central computer and sequencer (CC&S) MT-8 or MT-9 commands as well as the DC-26 ground command to turn off all science instruments.

The other reason for the switching change was the revision in purpose of the CC&S MT-8 command. On *Mariner* Mars 1964 this command served to turn off the encounter science instruments and the non-real-time DAS after encounter. On *Mariner* Venus 67, however, its purpose was

to switch the science and DAS to the encounter mode (data mode 3) and enable the planet sensor. For these reasons, the power distribution assembly was modified so that neither the CC&S MT-8 or MT-9 commands affected science power. The MT-8 command was no longer used by the power subsystem.

The functions of the DC-25 and DC-26 ground commands, which served on *Mariner* Mars 1964 as a backup to the CC&S MT-7 and MT-8 commands, respectively, were also revised. None of the science complement on *Mariner* Venus 67 is encounter oriented; consequently, all of the science instruments are on throughout the flight. The DC-25 command, which became DC-V25, serves not only as a backup to the MT-7, but also provides the override of the exclusive circuit previously described. In addition, this command turns the science power on through a redundant relay and turns the battery charger off as it did on the *Mariner* Mars 1964 spacecraft. The function of the DC-V26 command is to: (1) reset all the magnetic latching relays for science power (separation, DC-2, and DC-25), and (2) turn the battery charger off. In addition to these functions, the command also serves as a reset for the exclusive circuit override command DC-V25. One other command on *Mariner* Mars 1964 turned science off; this was the data encoder command (data mode 4) for the tape playback. This was not required on *Mariner* Venus 67 and, thus, was eliminated from the power subsystem.

Another change was made to facilitate the command sequences. In *Mariner* Mars 1964, the DC-28 command only turned on the battery charger; it had to be turned off by either a DC-25 or DC-26 command. For *Mariner* Venus 67 the switching logic was revised to allow the DC-V28 command to sequentially turn the battery charger on or off (toggle) by sensing its state at the time the command is given.

During the flight of *Mariner IV*, the battery terminal voltage continued to rise after the charger was turned off. It is theorized that this was caused by the mechanization of the battery voltage monitor, which allowed a small trickle charge current of approximately 1.6 mA to flow into the battery continuously. For *Mariner* Venus 67 the battery was isolated from the voltage monitor circuitry by an emitter follower circuit.

2. Testing. After completion of the modifications to the power conditioning described above, the flight and flight spare units underwent system testing on the spacecraft. Concurrently, the TA unit underwent testing.

The spacecraft testing of the power subsystem proceeded satisfactorily, with only a few difficulties occurring. One was associated with the addition of the dual frequency receiver (DFR) experiment to the spacecraft for the *Mariner* Venus 67 mission. This receiver uses two frequencies, 50 and 420 MHz, for its operation. During the system testing, the power subsystem booster regulator was one of the major sources of 50-MHz noise on the spacecraft, and interfered with the DFR. Experience with the B/R on *Mariner* Mars 1964 had shown that there were noise spikes generated in the subsystem, but these had not caused any major interference to other subsystems. A source of this noise was known to be the diodes in the power rectifier section of the B/R. Replacement of these diodes with a newer type substantially reduced the 50-MHz noise.

Another difficulty which occurred during system testing was related to the modification made to allow the DC-V28 command to be toggled. The circuitry is covered in detail in Section IV. However, when the charger was in the boost enable mode, and the boosting started, the effect was as though a DC-V28 command had been given and the battery charger switched from boosting to charging. This did not allow boosting to occur as desired. The difficulty was resolved by adjusting the value of two resistors in the toggle circuit.

A third difficulty which occurred during system testing was associated with an operational support equipment (OSE) function. Twice during electrically quiet periods of system testing on the flight spacecraft, the OSE lights, indicating whether the spacecraft is operating from internal or external power, came on simultaneously. Each time this occurred the power subsystem had been on the internal position of the power transfer switch; no change was noted in the position of the switch, nor in the source of spacecraft power. At first it was thought that the difficulty was caused by foreign material in a junction box of the system test complex. However, when it occurred the second time, the current on the external power indication line was traced to the spacecraft. Unfortunately, it disappeared during troubleshooting. After the second occurrence of this phenomenon, tests were run on the spacecraft to evaluate ground integrity and to check for a pin-to-pin short in the spacecraft umbilical connector or harness. Response time and leakage tests were also made on the power transfer switch and Case VIII, which contains the switch. None of these tests revealed anything that could have caused the difficulty. It never recurred, either in the remainder of the system testing or on the

launch pad, nor was any difficulty experienced in transfering from external to internal power or back.

All of the power subsystem modifications were thoroughly tested in the systems testing, including the exclusive circuit and the exclusive-circuit override command. No difficulties, other than those discussed, were noted. The TA testing for *Mariner* Venus 67 proceeded well even though this unit had undergone TA testing and 8300-h of life testing on the *Mariner* Mars 1964 program. The life testing on *Mariner* Mars 1964 had been terminated because of a catastrophic failure of a filter capacitor in the 400-cycle, 3-phase inverter. These capacitors were replaced during the rework for *Mariner* Venus 67 and the case assembly was undergoing electrical tests prior to flight approval (FA) thermal-vac when one of the replacement capacitors failed. Both failures were traced to electrolytic leakage around the terminal seal of the capacitor. These capacitors were subsequently replaced in all of the 400-cycle, 3-phase inverter subassemblies with capacitors of identical value, but improved seal design. No further difficulties were experienced with this type of capacitor.

C. Battery

1. Design. The only problem noted with the *Mariner IV* battery was the increasing terminal voltage after termination of charge; this was attributed to the trickle charging by the voltage monitor circuitry. Because new batteries had to be fabricated, some minor improvements were instituted into the design.

In the *Mariner* Mars 1964 battery design, a vent hole had been left in the cell cover to aid in filling the cells with electrolyte. It was found that this vent hole was not used during the fabrication of the *Mariner* Mars 1964 batteries, therefore, this hole was eliminated in the cover design for *Mariner* Venus 67. This eliminated a weak spot in the cell seal and allowed a continuous seal between the cell cover and case.

The active material mix of the negative plate for the *Mariner* Mars 1964 battery consisted of 90% ZnO, 7% HgO, and 3% PVA binder. This binder had been changed from teflon powder to PVA for *Mariner* Mars 1964 in the expectation of some improvement. It was found that the improvement was not measurable and that the recombination rates of oxygen on the negative plate could be increased by a return to the teflon powder. This was done for *Mariner* Venus 67.

The third change made was not a change in materials, but in processes. On the *Surveyor* battery program, the uniformity and quality of the cellophane separator used in the plate wrap tended to vary significantly from lot to lot. The battery vendor had instituted increased inspection processes and acceptance criteria for the cellophane separator on *Surveyor* and this improved acceptance specification was used for *Mariner* Venus 67.

2. Testing. The battery chosen for flight did not undergo testing with the other spacecraft elements until the spacecraft was ready to be installed on the *Agena*. Batteries identical in design were used during the spacecraft vibration and space simulator testing. Spare batteries from *Mariner* Mars 1964 were used during the SAF testing. This was necessary because the average lifetime of a battery in use is 6 discharge-charge cycles. By only using the flight battery on the last system test, assurance is provided that the battery flown is in the best condition possible.

Because of this, the acceptability of the battery design and capability of the flight battery must be based on the tests of the TA batteries, the spacecraft tests using test batteries, and the FA tests and manufacturing data of the battery chosen for flight. One battery was initially procured as an engineering battery because the manufacturer had not fabricated this model since the *Mariner* Mars 1964 procurement. The engineering battery underwent TA testing as well as some additional special testing to determine specific battery characteristics.

Three batteries were bought for TA testing on the *Mariner* Venus 67 program. These were used to verify the design and the manufacturing capability. The TA batteries performed nominally during the testing, but all three had some occurrence of plate wire breakage as did the TA batteries on *Mariner* Mars 1964. However, two of the three batteries were accidentally shocked during vibration; because of the shock it was difficult to determine whether the plate wire breakage was entirely a result of the vibration or an effect of the shocking. The plate wire breakage had not been observed on any battery as a result of the FA vibration tests. Even with the broken plate wires, the capacities of the TA batteries were above the specification requirements at both +32°F and +140°F. The specific details of the testing and the capacities obtained are given in Section V.

There were two instances of cell leakage in batteries that were being used for SAF testing of the spacecraft. Both of these were spares left from the *Mariner* Mars 1964

program and were ~2.5-yr old at the time. Because of the age of these batteries this was not considered to be an unusual situation.

The performance of the system test batteries during spacecraft vibration and space simulator testing and the performance of the flight battery through midcourse has all been nominal.

D. Power Subsystem Flight Operation

The overall operation of the *Mariner* Venus 1967 power subsystem during the cruise and encounter of *Mariner V* followed expected characteristics. There were variations from the expected data in the outputs of the I_{sc} and I_{scr} (see Section III, G) experimental solar cells and in the solar panel temperature, but no failures were noted.

The battery was used twice during the mission: for launch and for the midcourse maneuver. The initial battery use started with the transfer to internal power at L − 7 min and continued until the sun was acquired about 30 min after liftoff. The battery was then recharged until the midcourse maneuver when the pitch turn caused a shading of one solar panel and sharing between the solar panels and battery. The battery was used for an additional 46 min at this time. When the sun was reacquired after completion of the maneuver, the battery resumed charging. The battery charger was turned off at L + 13 days.

The solar panels provided power for the spacecraft from sun orientation after the spacecraft/*Agena* separation until the maneuver, and throughout the remainder of the mission. Sharing of the solar panels and battery occurred during the maneuver as described above. Panel capability was estimated to be 405 W near earth and 615 W near Venus.

The power conditioning equipment functioned as designed throughout the mission with no anomalies. The power subsystem responded to and executed each command as expected.

III. Solar Panel Design and Test

The *Mariner* Venus 67 solar array was designed to meet the raw electrical power requirements and environmental extremes which would be experienced during the spacecraft mission to Venus. A basic ground rule associated with this design was that it would employ *Mariner* Mars 1964 technology wherever possible to minimize development schedule and cost. Functional requirements for the design of the solar array stipulated that it provide a minimum of 360 W of power at a space solar intensity of 135 mW/cm² and 58°C, that the voltage output from the array be limited to 50 V, that the voltage at maximum power should be 44 ±2 V, and that the panel weigh less than 15.7 lb.

The *Mariner* Venus 67 spacecraft solar array consists of four oriented solar panels each having 10.9 ft² of area available for solar cell mounting. The cell layout on each solar panel consists of a folded string (Fig. 1); after deployment it is maintained in a plane perpendicular to the Z-axis of the spacecraft. For improved reliability each panel is divided into 3 isolated electrical sections that consist of 2 folded strings of 105 cells in series and 14 cells in parallel. The solar cells used in the design are 1 × 2 cm P-on-N (P-N) silicon solar interconnected into 7-cell submodules with gold-plated Kovar bus bars. The output of each electrical section of the array was shunt regulated by a string of 6 zener diodes to limit the voltage output to less than 50 V. The electrical schematic of a typical electrical section is shown in Fig. 2. Basically, the electrical design is the same as that employed on the *Mariner* Mars 1964 solar panel. Similar materials, submodules, and techniques were incorporated wherever possible. Table 1 provides detailed information on the *Mariner* Venus 67 solar panel.

The cell layout and cable routing was designed to minimize the magnetic fields caused by solar-panel current flow and materials. The use of the folded electrical section concept minimizes the magnetic field generated by

Table 1. Solar panel description

Item	Quantity
Solar panel area	10.9 ft² (35.5 × 44.40 in.)
Total area per spacecraft	43.6 ft² (4 panels)
Cells per panel, including packing factor	404 cells/ft² × 10.9 ft² = 4410 cells
Cells per spacecraft	4410 × 4 = 16,640 cells
Submodule size, 2 cm × 7 cm	1 series × 7 parallel, *Mariner* C type
Number of submodules per panel	630
Number of submodules per spacecraft	630 × 4 = 2,520
Sections per panel	3 each, 105 series, 14 parallel
Panel matrix	105 series × 42 parallel, 3 sections
Spacecraft matrix	105 series × 168 parallel, 12 sections
Estimated power in earth-space	≈ 100 W per panel
Spacecraft raw power at near-earth space	≈ 400 W

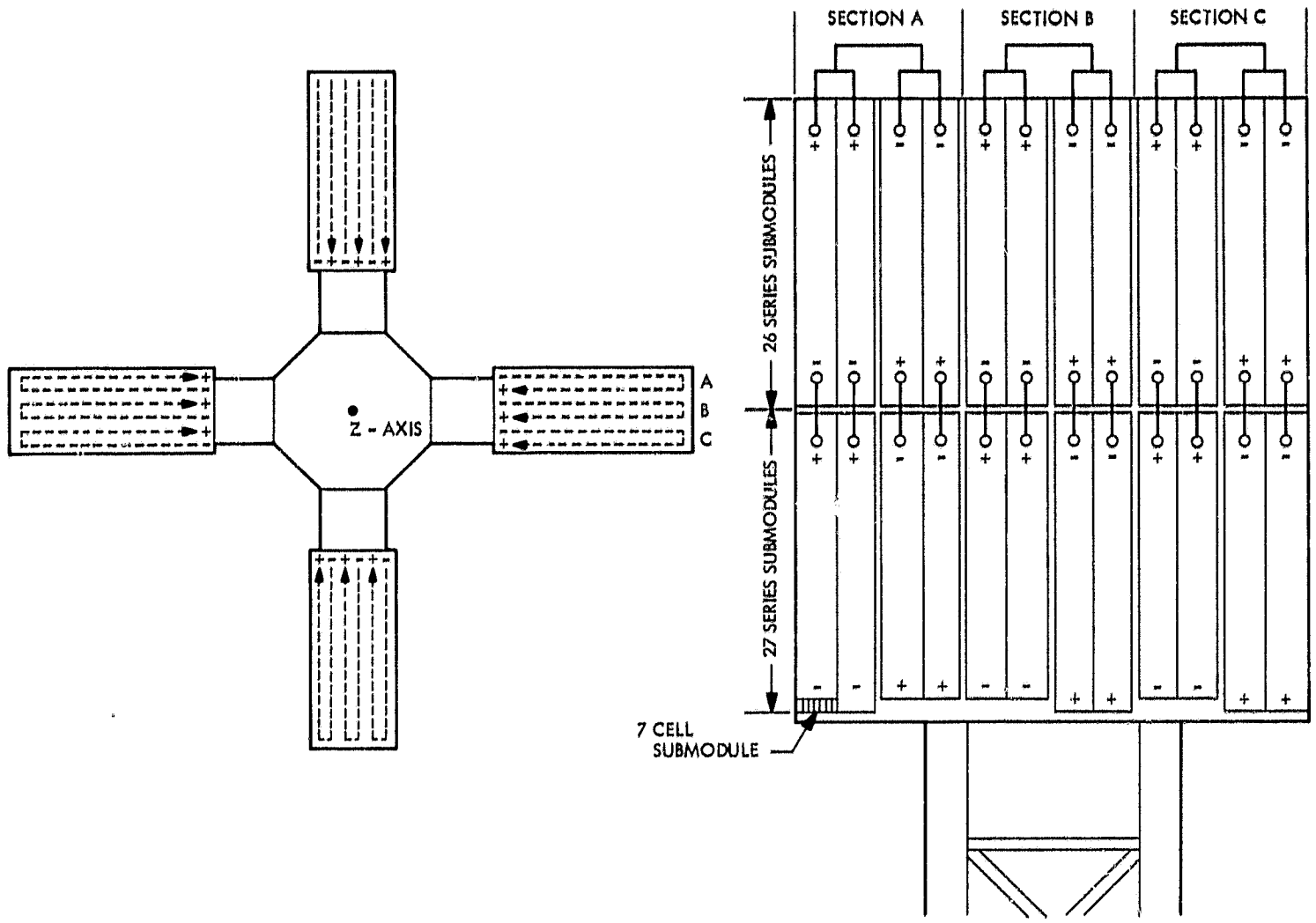

Fig. 1. *Mariner* Venus 67 solar panel

the solar cell current through cancellation caused by positioning adjacent current paths flowing in opposite directions. In addition, the voltage strings all terminate at the inboard edge of the panel, thereby greatly simplifying the cabling required. The longitudinal string orientation also reduces the possibility of the loss of a complete panel of three voltage strings resulting from shroud damage during the shroud separation event. To provide good heat sinking and radiation to space, the zeners were mounted on the supporting spars of the array structure.

Additional features of the *Mariner* Venus 67 solar array included four transducers to aid in monitoring the array operating temperature and a short-circuit current and open-circuit voltage transducer (Figs. 3–6).

A. Solar Panel Substrate Design

The *Mariner* Venus 67 solar panel substrate (Figs. 3 and 4) was contractor fabricated for JPL. The design consisted of a 4-mil aluminum skin reinforced with lateral 3-mil corrugations; this substrate matrix was supported over its entire length by 2 parallel box beam spars. The corrugation skin and spars were bonded together with an epoxy adhesive.

The vertical elements of the corrugation and the spars were pierced with flanged lightening holes to minimize weight and to aid in heat radiation from the back side of the skin. The entire back surface of the panel was coated with a high-emissivity gloss black paint. The cell surface of the substrate skin was covered with a 3-mil-thick epoxy impregnated fiberglass to provide an electrically insulating layer to mount the solar cells. The resulting solar panel substrate weighed ~9 lb.

Control of the panel's quality and safety during fabrication was strictly maintained by contractor and JPL inspectors. The substrate, which is loaded with solar cells and zener diodes to approximately the same weight as the substrate itself, could be seriously damaged by a

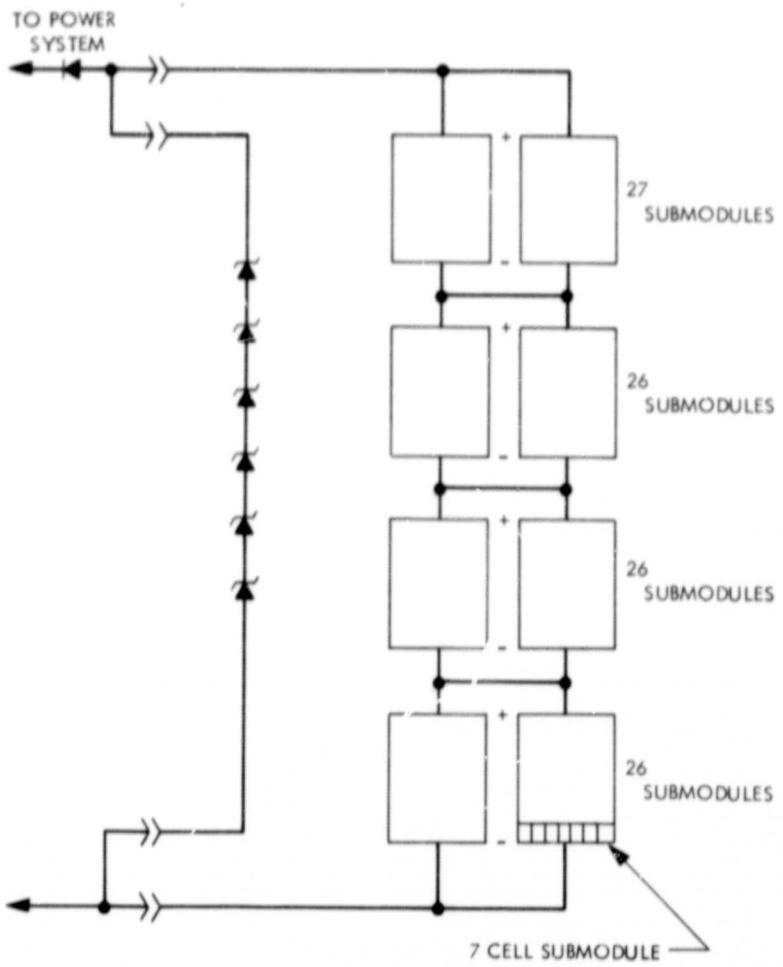

Fig. 2. Schematic of typical electrical section

pencil falling onto its surface from the shirt pocket of someone standing over it. After fabrication and before final acceptance, the solar array structure assembly was given a final thorough inspection by JPL quality assurance personnel to ensure dimensional tolerances. This included skin surface flatness, bond fillets, and dielectric strength of the insulating coating. It was also required that all panels be subjected to an ultrasonic inspection to ensure good adhesion of skin, corrugation, and spars.

B. Zener Diode Shunt Regulator

The flight configuration of the *Mariner* Venus 67 solar-array shunt regulator required 6 zener diodes connected in series for each electrical section of a panel. The diodes were torqued to the underside of the panel's box beam spars, which provide heat sink for controlling diode temperature in excess of the anticipated worst case power dissipation of 10.5 W/diode. The diodes were electrically insulated from the spars with 6-mil mica washers, and after installation were coated with nonconductive black paint to improve their surface emissivity.

The diodes had the following nominal characteristics: a zener voltage of 8.25V ±2% at 1 A, and a 90°C stud

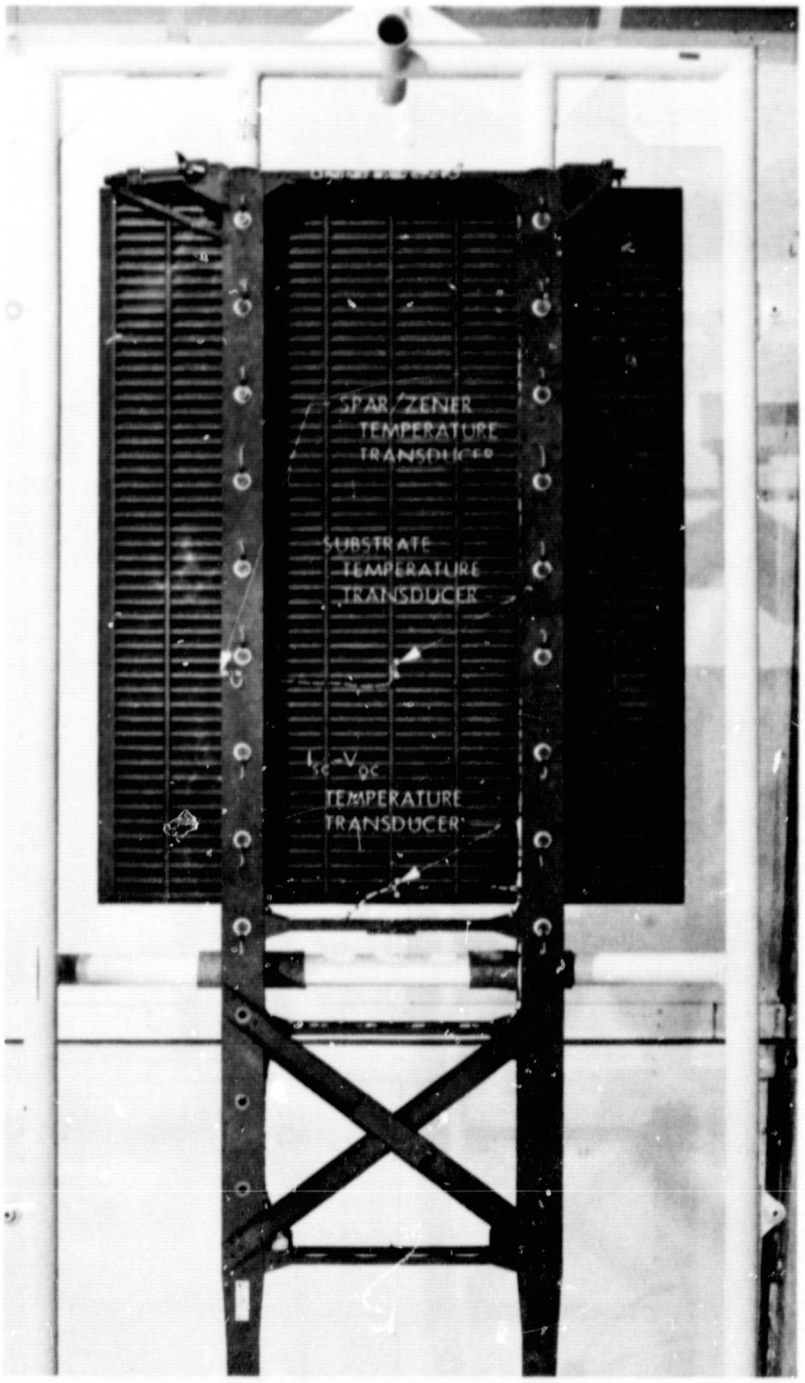

Fig. 3. Solar panel, rear surface

temperature with a temperature coefficient of 3.27 ±0.72 mV/°C.

C. Solar Cell Assembly

Boron diffused, 1 × 2 cm P-N, silicon solar cells with electroless nickel plating, solder-dipped ohmic contacts were employed in the *Mariner* Venus 67 array fabrication. Most of these cells were procured during *Mariner C*, although some additional cells were required for *Mariner* Venus 67. To effectively control the quality of the solar cells, a JPL source inspector witnessed 100% of the sample lot mechanical and electrical testing of each 5000-cell lot.

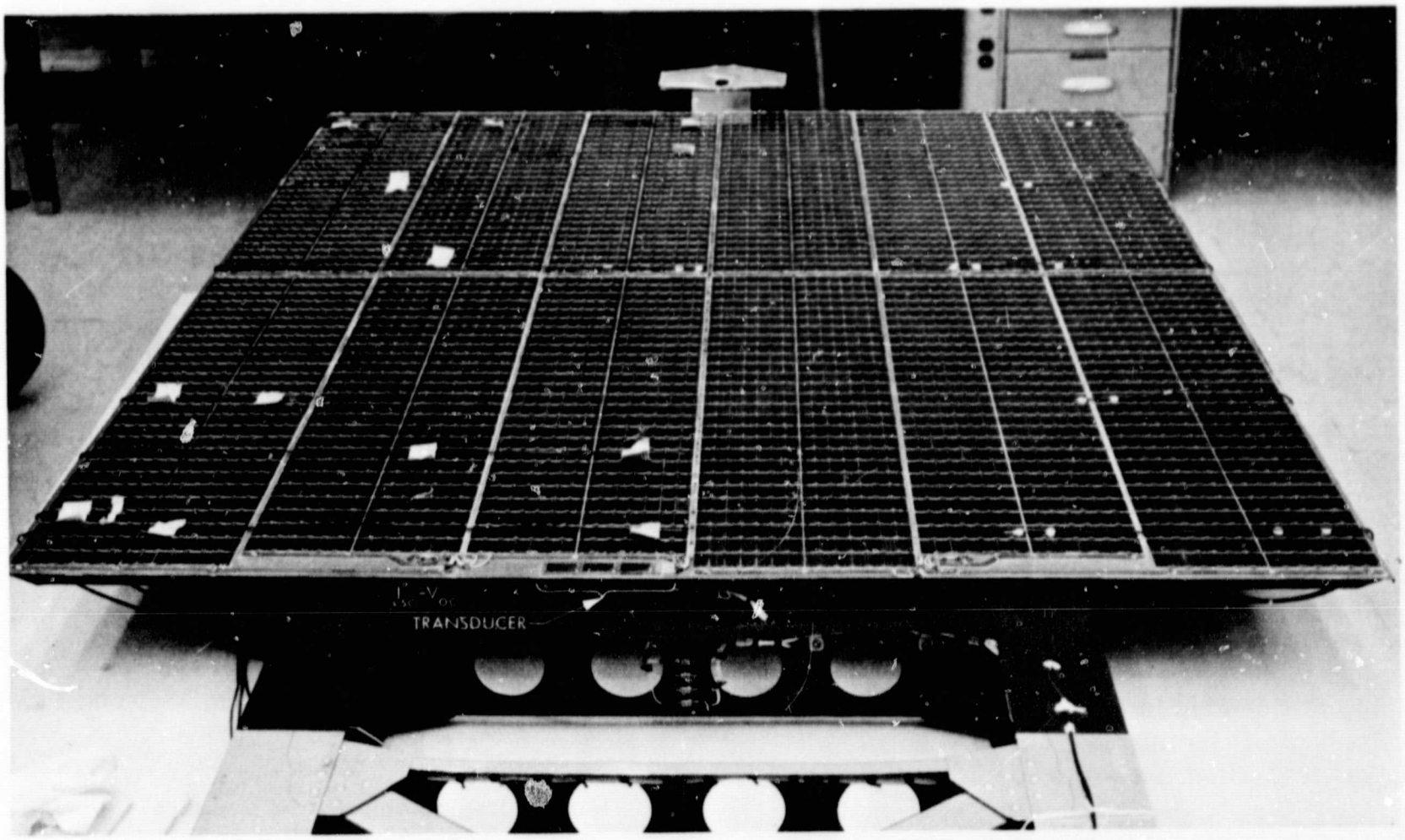

Fig. 4. Solar panel, front surface

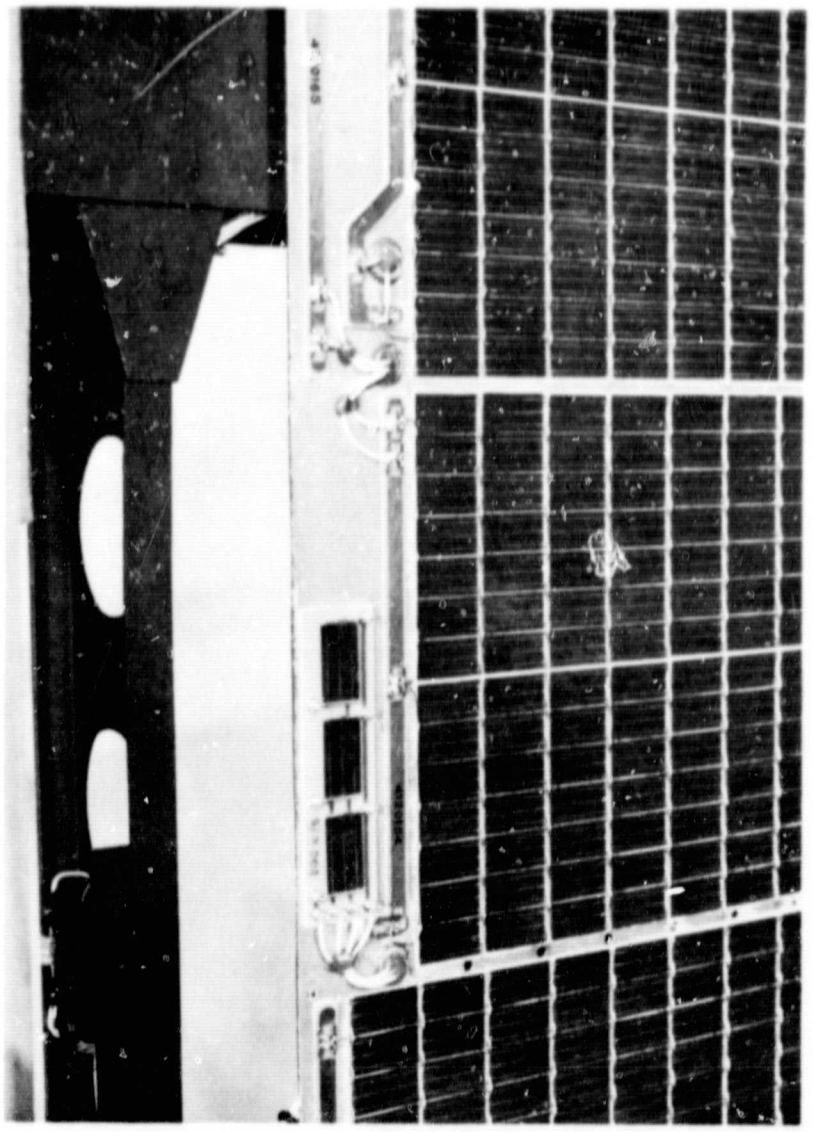

Fig. 5. Closeup of I_{sc}-V_{oc} transducer

Fig. 6. Closeup of typical temperature transducer installation

The solar cells were subjected to additional screening by an independent testing organization. The independent testing organization's function was to verify, on the same sample lot basis as that noted above, the power output and shape factor characteristics of each lot of cells and to environmentally test a 225-cell sample from each lot. This environmental testing consisted of ethylene oxide, thermal vacuum, thermal shock, temperature–humidity, and temperature soak. Electrical performance measurements of the cells were required before and after each test. Special tests were also conducted in the JPL photovoltaic laboratory on sample cells from each of the lots to evaluate the effects of temperature from −20°C to 150°C and intensities from 30 mW/cm² to 300 mW/cm² on the cells' electrical performances. A plot of the *Mariner* Venus 67 mean solar cell characteristics prior to and after filtering and assembly is shown in Fig. 7. The data are reduced to 100 mW/cm² tungsten data and are intended to show power loss due to assembly.

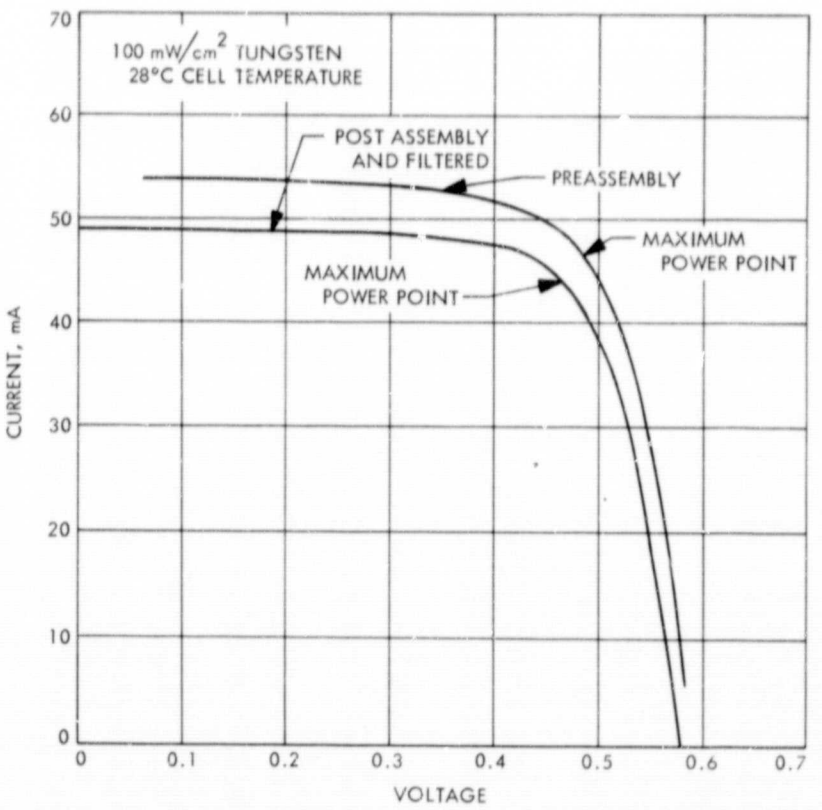

Fig. 7. Average individual solar cell current-voltage curves for *Mariner* Venus 67

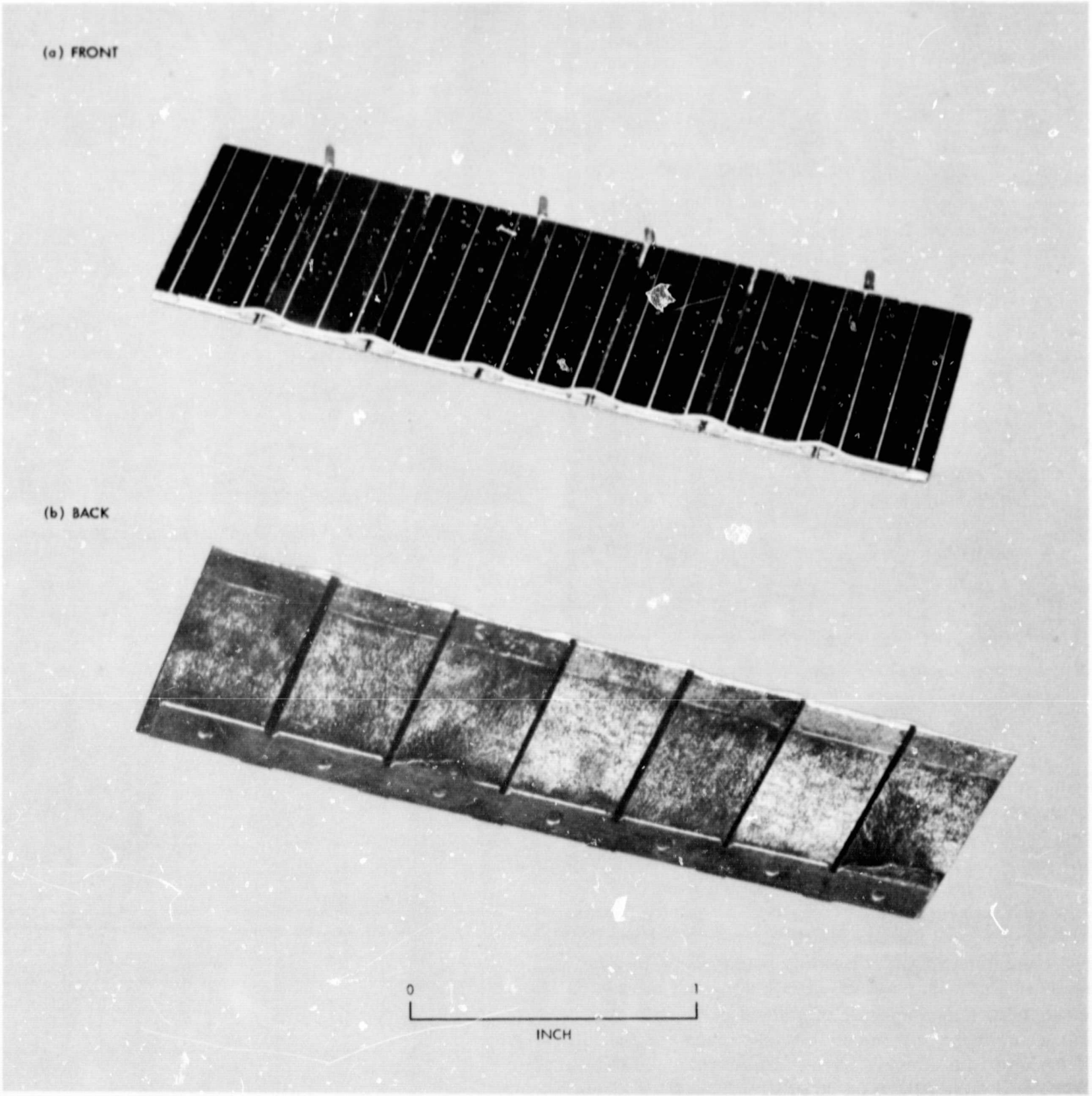

Fig. 8. Typical solar cell submodule: (a) front, (b) rear

D. Solar Cell Submodule

A solar cell submodule is the smallest subassembly of the solar array and consists of solar cells, filter covers, filter adhesive, and bus bars. The *Mariner* Venus 67 submodule solder connections were made directly to the cells before assembly of the submodule to the panel (Fig. 8). This design was used on *Mariner* Mars 1964 and permitted more meaningful evaluation of the electrical and mechanical characteristics of the individual submodules, thereby improving series string matching and QA inspection techniques. This significantly reduced the amount of work involved in the assembly of the submodules on the panel. The individual solar cells are electrically interconnected on the P side with a 20-mil wire and on the N side with a 3-mil-thick ribbon each of which was gold-plated kovar. Kovar is used because of its similar thermal coefficient to the silicon solar cell.

Each solar cell is covered with a glass filter to protect it from space low-energy radiation and to aid in temperature control of the cells during flight. The filter covers were fabricated from a 6-mil-thick Dow Corning 0211 microsheet substrate with a 0.410-micron cutoff filter vacuum deposited on one surface.

E. Solar Panel Submodule Manufacturing

JPL screened solar cells, filters, and adhesives were contractor fabricated into *Mariner* Venus 67 submodules. A semiautomatic process involving a tunnel oven was employed in soldering the solar cells and kovar bus bars. A tunnel oven with zone temperature control through which components are automatically conveyed is shown in Fig. 9. The tunnel oven could be controlled to optimize the time–temperature soldering cycle of a submodule to insure good solder bonds and minimize electrical degradation. The cells were assembled into a machined graphite fixture; this served to correctly position bus bars relative to the cells and fixed the critical maximum and minimum dimensions of the submodule (Figs. 10–12). This technique was successfully used on *Mariner* Mars 1964 hardware. The *Mariner* Venus 67 submodules were fabricated in a significantly improved tunnel oven. The oven was developed shortly before program initiation by JPL in an advance development effort to investigate improved solar panel fabrication technique.

F. Solar Array Temperature Monitoring

Four temperature transducers are used to aid in the evaluation of the space performance of the *Mariner* Venus 67 solar array. The temperature transducer selected for use on the *Mariner* Venus 67 solar array was a small

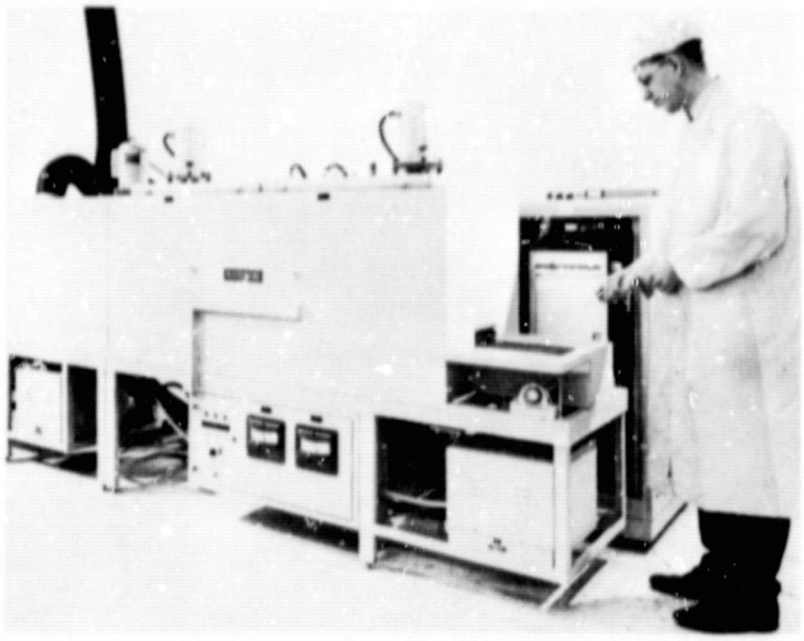

Fig. 9. Submodule tunnel oven

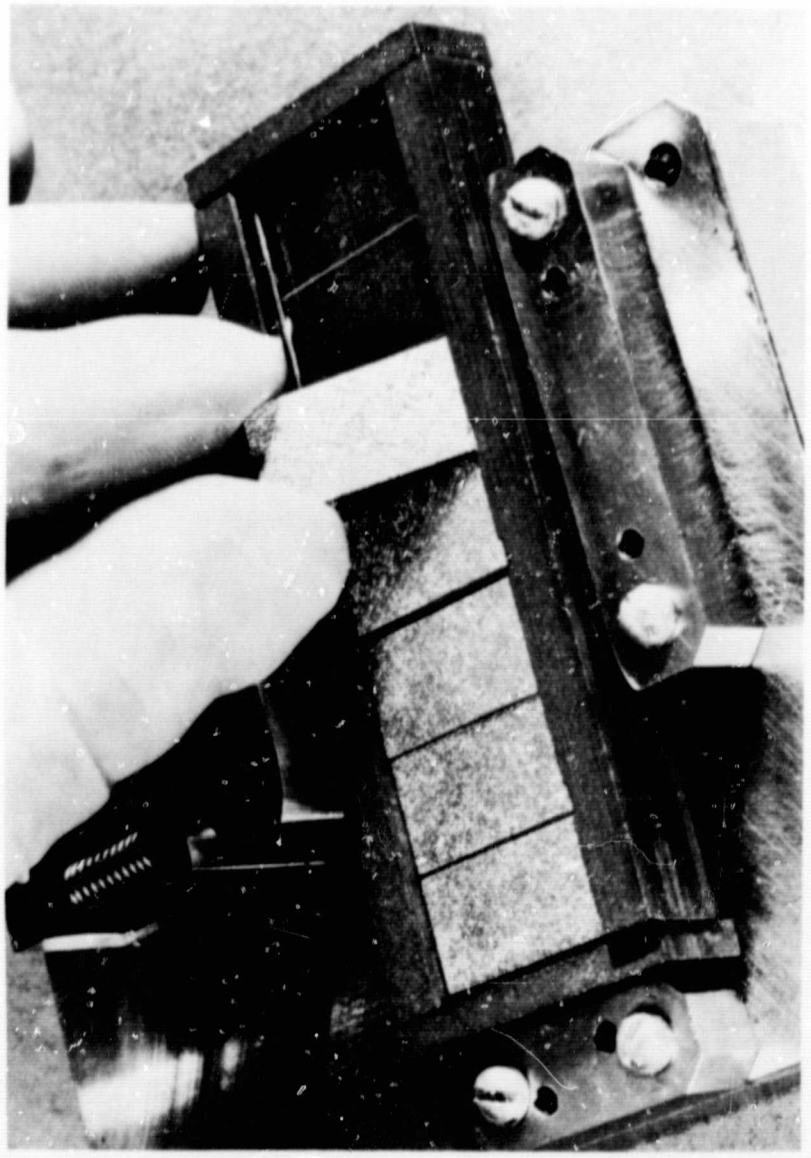

Fig. 10. Cell emplacement in the solder boat

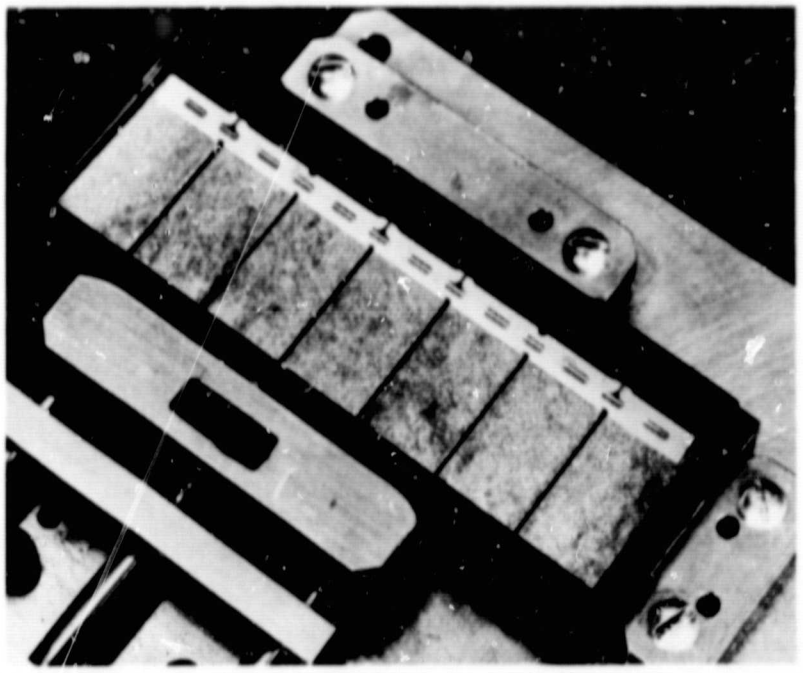

Fig. 11. Assembled cells and N contact bus bar in a submodule boat

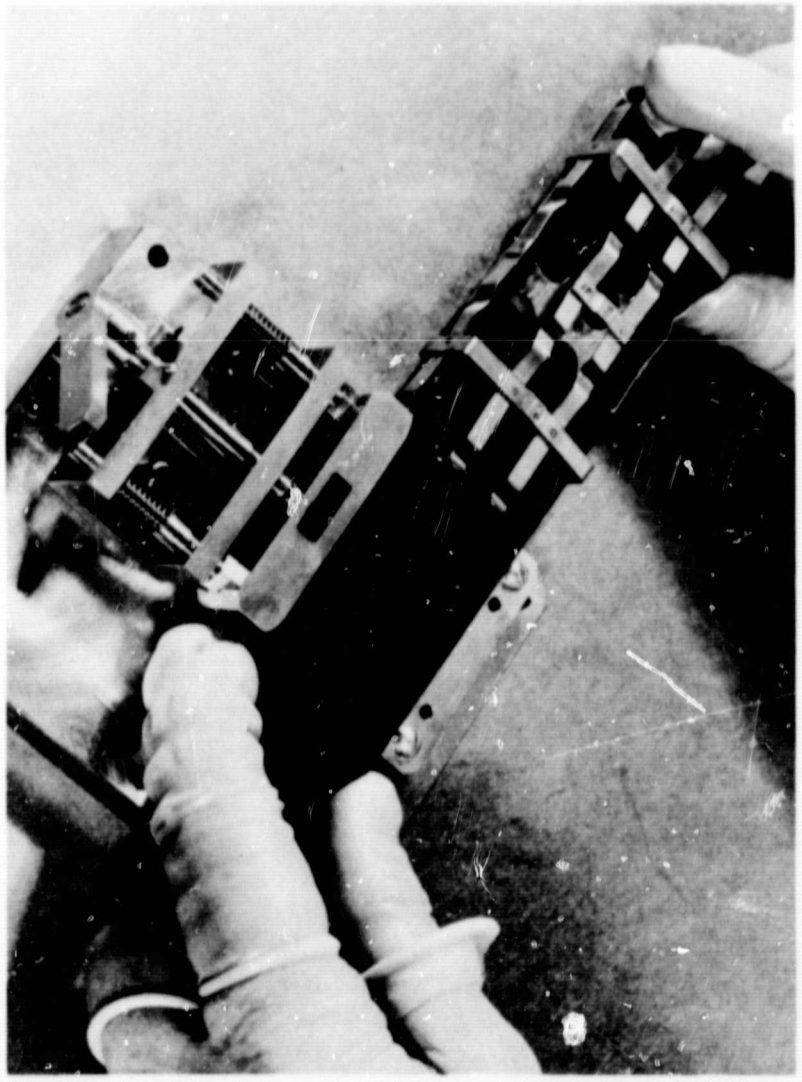

Fig. 12. Assembling the submodule solder boat

resistive element encased in a thin electrically insulating mylar jacket ~2-mils thick. The transducer exhibits a relatively linear resistance vs temperature range from plus to minus 300°F.

The transducers were procured and screened by JPL and supplied to the solar array manufacturer. Three transducers are actually bonded to each panel: one is in the center of the panel, one is under the short-circuit current-open circuit voltage (I_{sc}-V_{oc}) transducers, and the third is on the spar of the structure close to a zener diode (Figs. 3 and 6). In flight, only a total of four temperature transducers are monitored: the central unit on panels 4A1 and 4A5, and the I_{sc}-V_{oc} transducer and spar units on panel 4A5.

There are two other temperature dependent outputs on a *Mariner* solar array which can be used in evaluating the thermal equilibrium characteristics of the array: the open-circuit voltage cell of the I_{sc}-V_{oc} transducer, and the operating points of the solar array when the array is not limited by the zener diode shunts. These outputs, when compared to the preflight calibrated Voc cell and voltage-current characteristics of the array, help to give a relative setting to the space array temperature.

G. I_{sc}-V_{oc} Transducer

The I_{sc}-V_{oc} transducer's purpose is to aid in flight evaluation of array performance. The transducer is made up of three 1 × 2 cm *Mariner* '67 solar cell assemblies. Two of the assemblies were instrumented to monitor their short-circuit current outputs, the remaining cell was instrumented to monitor its open-circuit voltage (V_{oc} cell). One of the two short-circuit current cells used in the transducer was bombarded with 1 MeV electrons to ~ 10^{15} electron/cm² total flux level before assembly (I_{scr} cell). This radiation dose degraded the short-circuit current output of the cell ~ 50%, making it relatively insensitive to further radiation degradation. It then serves as a good space radiation damage indicator, when compared to the performance of the short-circuit current cell not subjected to preflight radiation damage.

The I_{sc}-V_{oc} transducer assembly was fabricated by JPL and supplied to the array manufacturer. The transducer was located at the spacecraft bus end and near to the center of the panel. Preflight calibration of the I_{sc}-V_{oc} transducer cells required intensity and temperature calibration under 2800°K tungsten illumination and sunlight at the JPL Table Mountain test facility. The cells were standardized on a JPL balloon flight. The cells are flown at 80,000 ft and the output of the cells in sunlight is

telemetered to earth. These cells are later recovered and incorporated into the I_{sc}-V_{oc} transducer.

H. Solar Array Assembly

Solar cells, substrates, zener diodes, and transducers procured and screened by JPL were supplied to the contractor for assembly into solar panels. One TA and six flight panels were fabricated and tested for this program. An elaborate quality control and manufacturing process control system was established which required frequent in-process inspection by both contractor QA and JPL resident inspectors.

The submodules were bonded to the front surface of the panel with a silicon adhesive, and interconnected in three sections as previously indicated. The 3 electrical sections per panel represent a total of 1,470 solar cells per section, 4,410 cells per panel, and 17,640 cells for a *Mariner* Venus 67 vehicle.

Bondable Teflon wire (22 AWG gauge) was used to connect the solar cell sections to the panel connector. The harness was routed along both inboard edges of the substrate spars and supported with Teflon cable clamps. All feed through holes for connections of the harness to the submodules were at the bus end of the panel. Connecting wires were branched from the main bundle, attached to the spars across the panel, and passed through these holes. The wire was protected by a teflon grommet.

To minimize the requirement for feedthrough holes in the panel and to reduce mechanical stress associated with the attachment of the harness cable directly to the submodules, a conformal coated printed circuit board concept was developed. The circuit boards provided all the intersubmodule redundant wiring required and were bonded to the front surface of the substrate.

I. Environmental Qualification Testing

Qualification of a *Mariner* Mars 1964 solar array required successful completion of a TA test program; this included vibration, thermal vacuum, acoustic noise, and humidity. All solar panels to be designated as flight hardware had to successfully complete a vibration and thermal vacuum FA test program. Evaluation of the effects of the test on a solar panel was accomplished by a comparison of the normalized electrical performance characteristics made in sunlight before and after each test at the JPL Table Mountain test facility and by 10-power microscopic inspection of all the panel assemblies and solder connections.

The TA solar panel successfully passed the vibration and acoustic tests; however, during the thermal vacuum test, which was conducted in the JPL 10-ft space simulator, a loss of electrical power to the solar simulator occurred. At this time the panel had been subjected to thermal shocks simulating midcourse maneuver at two sun–spacecraft distances less than L + 30 days and was exposed to a 60-h soak at 285°F. Light source power failure occurred after 48 h of high-temperature soak. This failure caused a severe thermal shock to the panel. After removal from the chamber, an electrical and mechanical inspection of the panel revealed that 16% of the solar cells showed P-contact delamination and that the electrical power output capability of this panel had decreased ~27%.

An extensive testing program was conducted to provide additional information to evaluate the mechanism and mode of failure. Twelve 1-ft² sample solar panels were fabricated and tested under varying thermal shock and thermal soak conditions. The resulting data strongly indicated that the TA panel would have successfully survived the thermal vacuum tests with probably no broken cell contact if the power to the solar simulator had not failed. A thermal shock of the type to which the TA panel was exposed would not normally occur in flight. Subsequent real-time life tests of two 1-ft² solar panels in a thermal vacuum environment profiled to look like the anticipated *Mariner* Venus 67 mission to E + 30 days showed no failures or design inadequacies.

It was anticipated that all flight solar panels would be FA vibration qualified as individual subassemblies before delivery to SAF and spacecraft FA testing. During the FA testing program it was quite difficult to test individual solar panels by vibration with confidence. The panels, when on the spacecraft, are tip latched; therefore, one supports and acts on the other during vibration. It was found that there could be significant variation in the response from panel to panel and that there was constant concern for overtesting. Midway through the FA vibration test program, it was decided to forego individual panel vibration qualification and to use the spacecraft vibration test to certify the mechanical integrity of each panel. No difficulties or abnormalities were encountered in using this process for the remainder of the program.

J. Predicted Array Thermal Characteristics

The design of *Mariner* Venus 67 is very similar in construction and material to that of *Mariner* Mars 1964.

Therefore, the preflight temperature data and analysis of *Mariner* Mars 1964 would, in most cases, be directly applicable to *Mariner* Venus 67. Because of the spacing between the inboard edge of the substrate and the spacecraft bus, the lengthwise temperature gradient due to bus-substrate interaction would be negligible. Presented in Figs. 13–16 are the predicted flight temperature conditions of the array, including the anticipated temperature rise expected to be experienced by the array during encounter due to Venus albedo and the transient conditions predicted for the array during a worst-case type of midcourse maneuver. *Mariner* Mars 1964 flight data generally supported the fact that the temperature of this array could be nominally described as resulting from a thermal analysis for a simple flat plate, where the area of the front surface of the panel effectively equals the area of the rear as shown in the following equation:

$$T = \left[\frac{H\alpha - P}{\sigma(E_f + E_r)}\right]^{1/4}$$

where

T = temperature in °K

H = normal solar intensity

P = solar energy converted to electrical energy

σ = Boltzmann's constant

α = hemispherical absorptivity of the front of the panel

E_f = hemispherical emissivity of the front of the panel

E_r = hemispherical emissivity of the rear of the panel

Based on *Mariner* Mars 1964 experience, α is assumed to be 0.83 $E_f = 0.79$, and $E_r = 0.90$.

K. Electrical Performance Testing

All electrical performance tests of *Mariner* Venus 67 solar panels were conducted at the JPL Table Mountain Test Site located 7,000 ft above sea level, near Wrightwood, California. The panels were oriented normal to sunlight and the current-voltage characteristic of each of the electrical sections was measured in the ambient temperature-humidity environment. The relative space intensity of the sunlight at the time of testing was monitored by a balloon flight-standardized calibrated solar cell, which had similar spectral response characteristics to the solar cells on the panel. The temperature of the panels was determined from the open-circuit voltage output normalized to some nominal intensity and compared to calibration curves relating voltage and temperature.

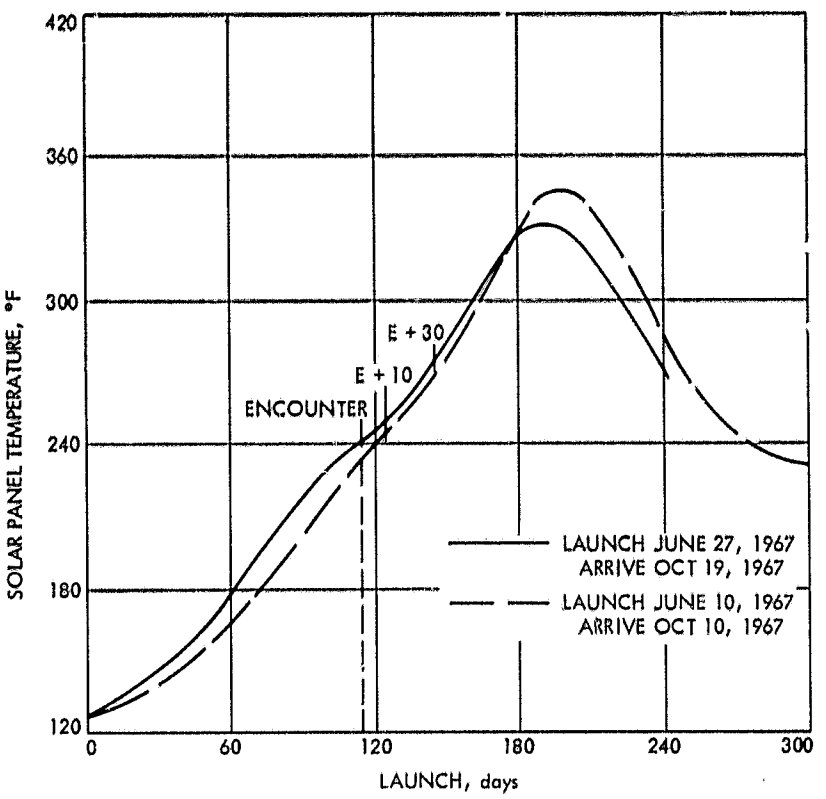

Fig. 13. Predicted solar panel temperature during Venus mission

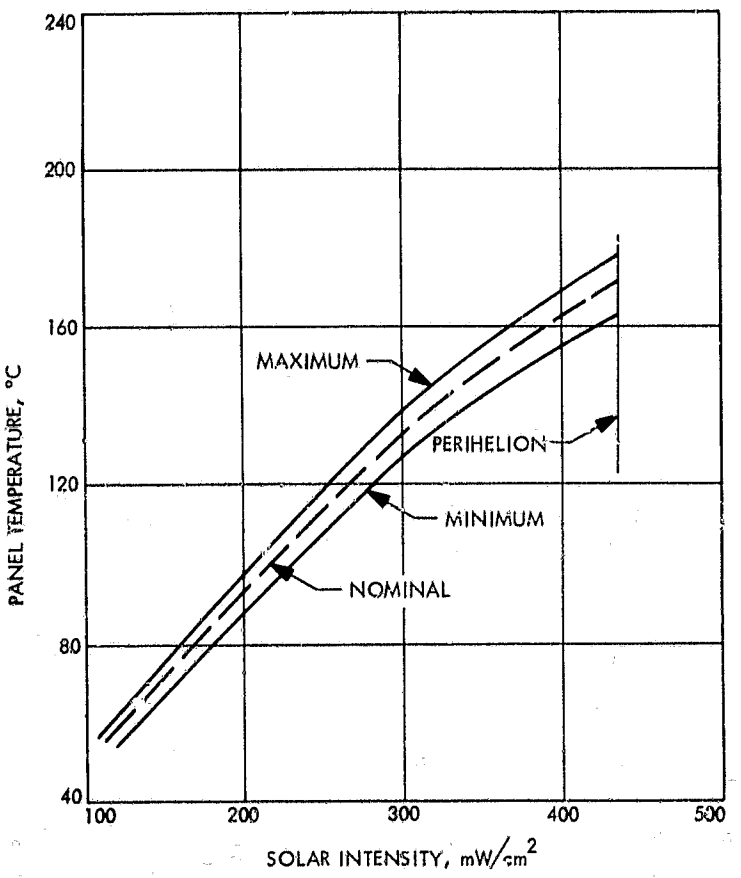

Fig. 14. Predicted *Mariner* Venus 67 solar panel temperature vs solar intensity

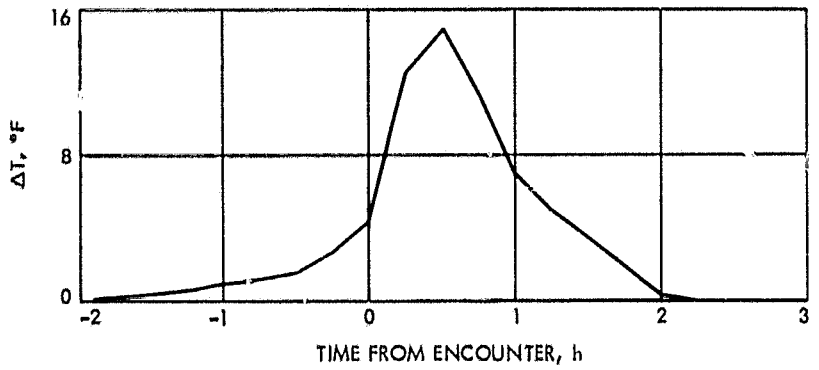

Fig. 15. Solar panel temperature rise induced by Venus

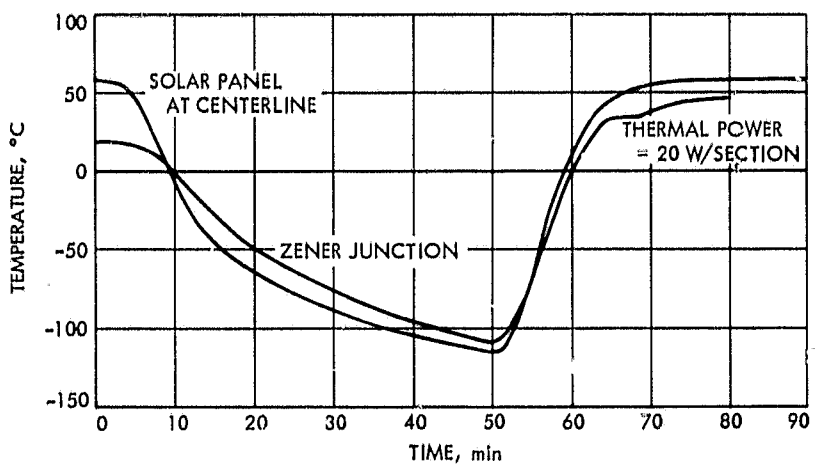

Fig. 16. Midcourse maneuver temperature history for *Mariner* Venus 67

The equation used to reduce solar panel data to space conditions is shown in Fig. 17. A summary of the electrical performance of the six *Mariner* Venus 67 flight panels is presented in Table 2. The data does indicate

Table 2. *Mariner* Venus 67 solar panel[a]

Panel position on flight spacecraft	Panel section	Power: maximum power, point-W	Voltage: maximum power, point-V	Short circuit current, A	Open circuit voltage, V
003	A	32.59	43.74	0.833	56.73
(spare)	B	33.31	45.26	0.832	56.73
	C	33.42	43.88	0.849	56.64
004	A	34.00	44.84	0.857	56.69
(spare)	B	33.80	44.51	0.851	56.69
	C	33.56	44.96	0.847	56.68
005	A	34.02	44.73	0.844	56.69
(4A5)	B	33.90	45.03	0.848	56.69
	C	34.01	45.42	0.850	56.69
006	A	33.55	44.16	0.841	56.67
(4A7)	B	33.67	44.84	0.843	56.69
	C	34.00	44.42	0.848	56.69
007	A	34.09	44.56	0.852	56.69
(4A1)	B	34.17	45.29	0.854	56.69
	C	34.05	44.93	0.854	56.67
008	A	34.04	45.22	0.845	56.69
(4A3)	B	34.12	45.73	0.849	56.69
	C	34.16	44.42	0.850	56.69

[a]Data reduced to 135 mW/cm² and 58°C.

$$I_2 = I_1 + I_{sc_1}\left(\frac{L_2}{L_1} - 1\right) + \alpha\left(T_2 - T_1\right)$$

$$V_2 = V_1 - \beta\left(T_2 - T_1\right) - \Delta I_{sc} R_s - K\left(T_2 - T_1\right) I_2$$

$$\Delta I = \Delta I_{sc} = I_{sc_1}\left(\frac{L_2}{L_1} - 1\right) + \alpha\left(T_2 - T_1\right)$$

$$P_2 = I_2 V_2$$

Where:

$$\alpha \equiv \left.\frac{dI_{sc}}{dT}\right| \text{intensity constant}$$

$$\beta \equiv \left.\frac{dV_{oc}}{dT}\right| \text{intensity constant}$$

Where:

I_1	Reference current coordinate
V_1	Reference voltage coordinate
I_{sc_1}	Short circuit current of the reference data
I_2	Extrapolated current coordinate
V_2	Extrapolated voltage coordinate
L_1	Reference incident solar intensity
L_2	Equivalent solar intensity to be investigated
T_1	Reference cell temperature
T_2	Cell temperature to be investigated
R_s	Panel effective series resistance
K	Series resistance correction function for temperature
α	Short circuit current temperature coefficient
β	Open circuit voltage temperature coefficient

Fig. 17. General equations used in determining the intensity-voltage characteristics of a *Mariner* Venus 67 solar panel

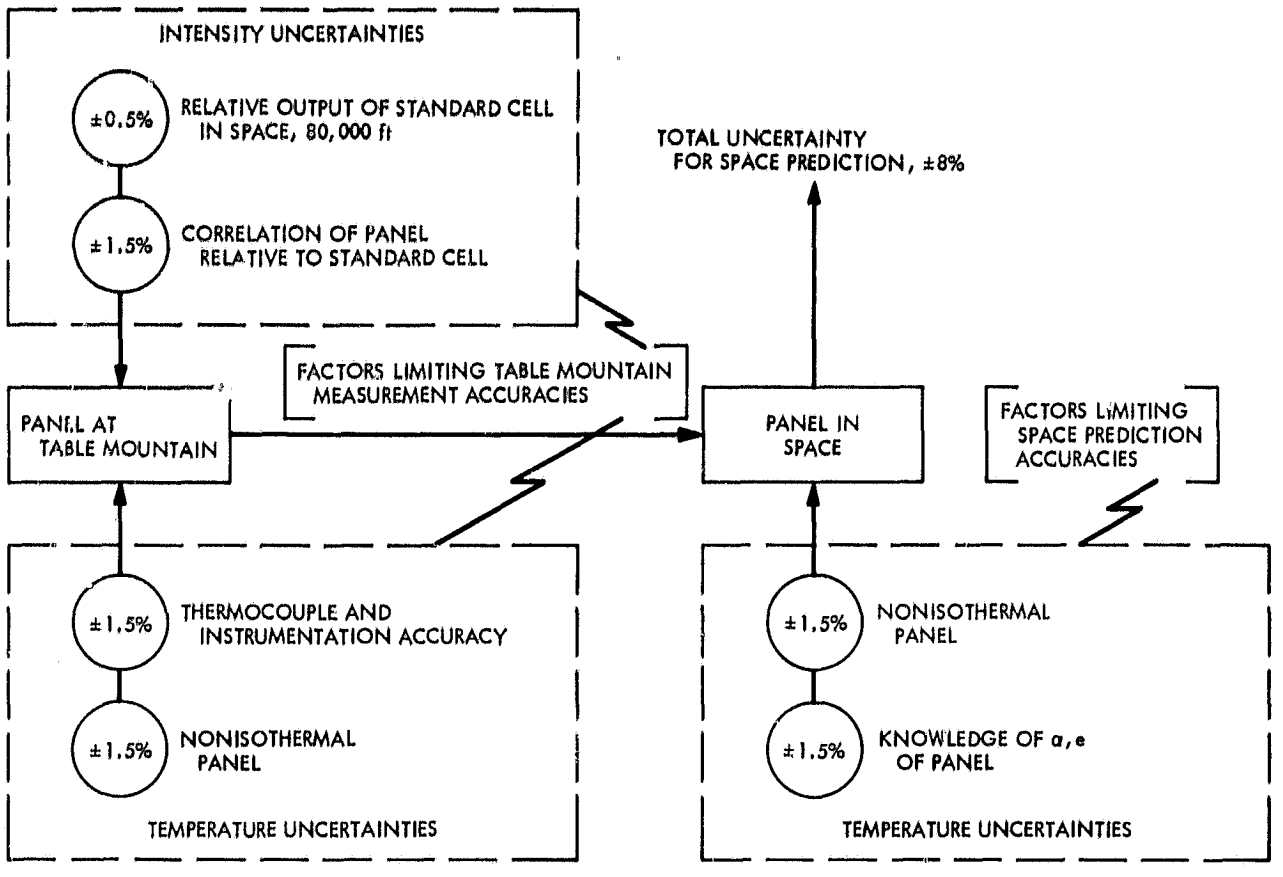

Fig. 18. Absolute space power capability contingencies prediction capability for a panel in space at some heliocentric distance based on Table Mountain predictions

that the panels, particularly the four flight panels, are relatively uniform. The uncertainties in predicting the performance characteristics of a solar panel in space based on Table Mountain measurements is assumed to be 8%. The causes of this uncertainty are displayed graphically in Fig. 18 and are primarily associated with measuring and predicting solar panel temperature.

L. Electrical Performance Characteristics

The predicted preflight electrical characteristics of the array are shown in Figs. 19–21. Incident solar intensity at the time of launch was calculated to be 135 W/cm² and the resulting temperature, based on *Mariner* Mars 1964 data, 56°C. From preflight measurements, it was determined that an undegraded *Mariner* Venus 67 solar array should have a power-temperature correction factor of ~0.32%/°C. Curves of an undegraded *Mariner* Venus 67 array showing maximum power output and voltage at maximum power as a function of heliocentric distance are presented in Figs. 19–21. Because of the zener-diode limiting during the early stages of the flight, the output voltage of the array will probably be determined by the zener diodes (Fig. 21). Assuming nominal performance and a cruise spacecraft load of 200 W, it is anticipated that the zeners will determine the voltage output until a panel temperature of ~80°C (176°F) is reached. Prior to this, the panel output voltage should vary only slightly. After this period, larger variations should be expected. Prior to launch, a last electrical check of the solar array was made at the Air Force Eastern Test Range (AFETR). A raw data curve of the solar panels obtained from these measurements is shown in Fig. 22. The data was then normalized to space sunlight conditions, and the output capability was compared to reduced data of the solar panels when last measured at Table Mountain. This data is presented in Fig. 23 and shows agreement to within 2%. Considering the AFETR test conditions and limitations of resolving data, the results were considered to support the conclusion that the panels appeared undamaged or undegraded and ready for flight.

M. Solar Panel Flight Operation

After the successful launch and separation of the *Mariner* Venus 67 spacecraft, early telemetry data of the solar panel characteristics indicated that the array was performing well. Two deviations from predicted data were noted, however. First, the solar panel substrate temperature after L + 5 days was approximately 7°C cooler than had been estimated. Second, the outputs of the I_{sc} and I_{scr} cells were approximately 3% higher than expected.

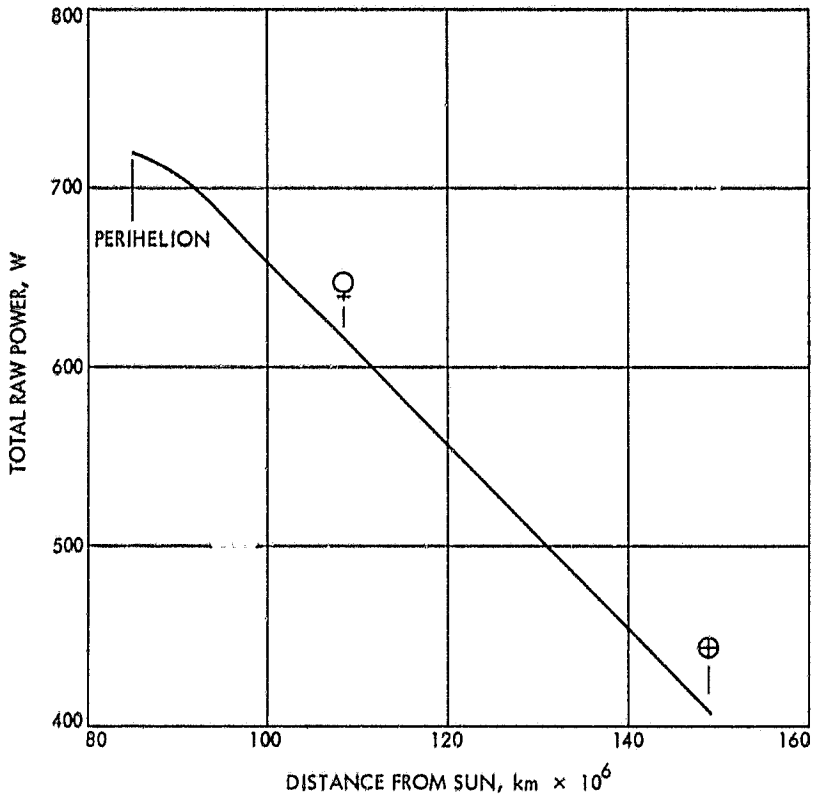

Fig. 19. Total undegraded spacecraft solar panel peak raw power vs heliocentric distance

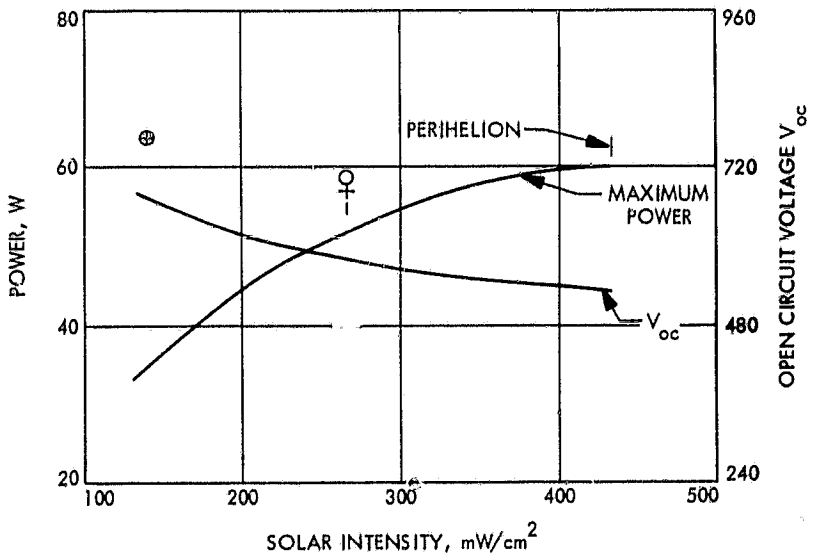

Fig. 20. Variation of panel section performance with intensity; for array characteristics the power is multiplied by 12

While this data was felt to be within the limits of prediction capability and the resolution of the telemetry system, a detailed study was initiated to reevaluate the preflight panel analysis.

The study of the 7°C temperature differential revealed that the original temperature predictions, based on an assumed power usage from the array, were somewhat

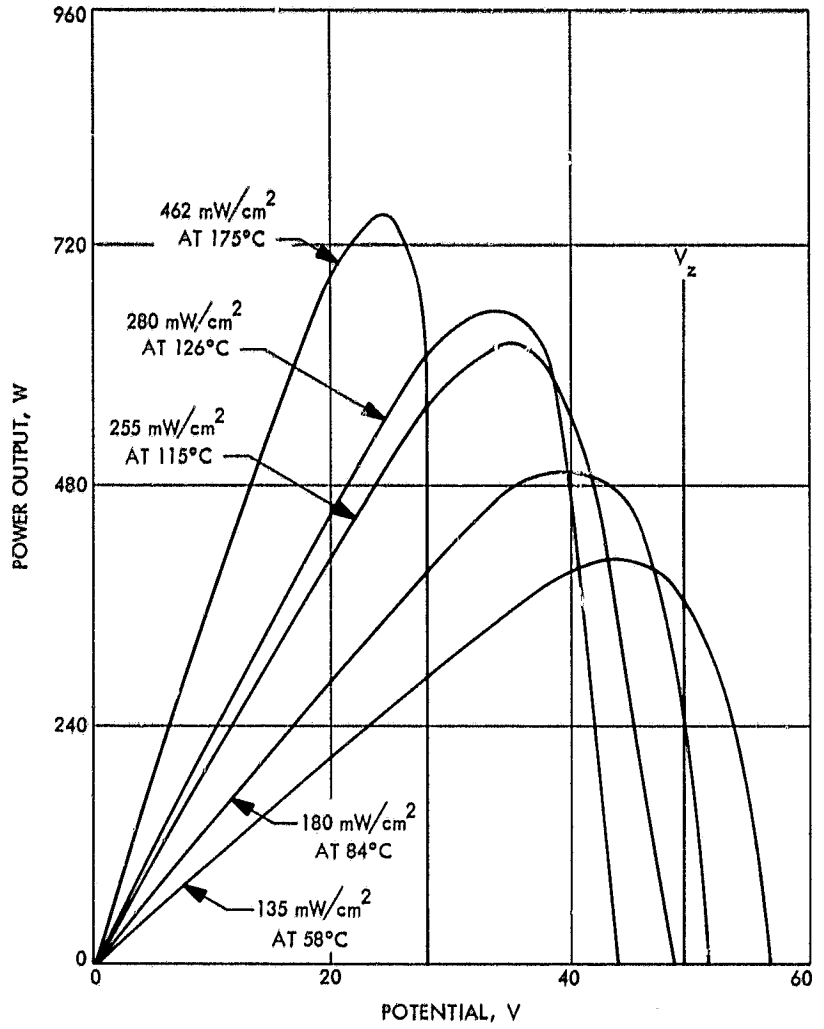

Fig. 21. Total panel power vs voltage for various conditions

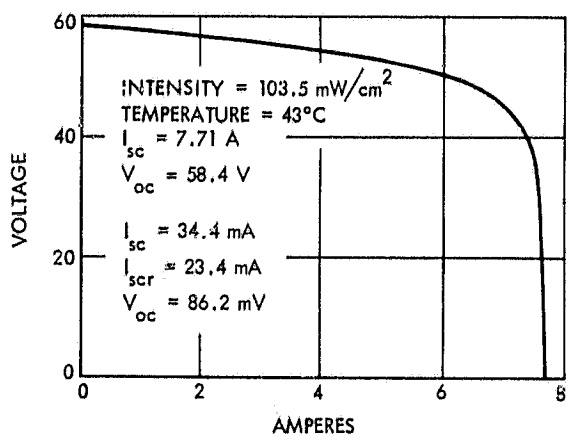

Fig. 22. Raw data curve for *Mariner* Venus 67 solar panels: solar panel intensity-voltage curve

lower than actually experienced. The spacecraft power requirements were well known from system test data. However, the operating point of the zener diodes, and consequently the power which they dissipated, was higher than had been predicted. During the near earth portion of the flight, the operating voltage of the zener shunts

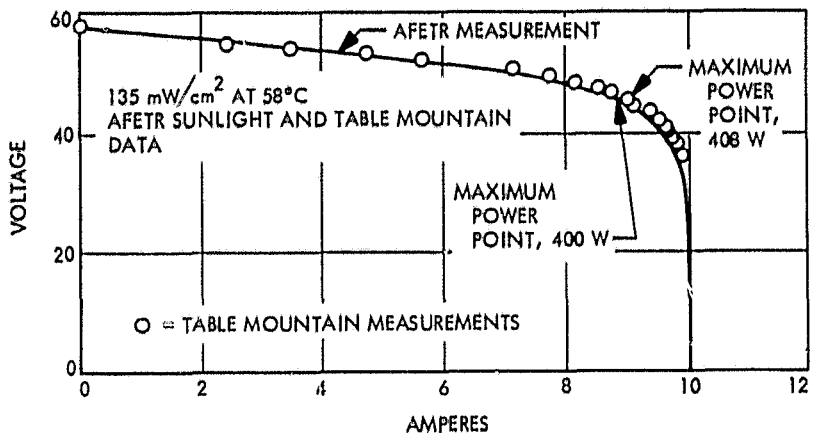

Fig. 23. Solar array reduced data for *Mariner* Venus 67 voltage-intensity curve

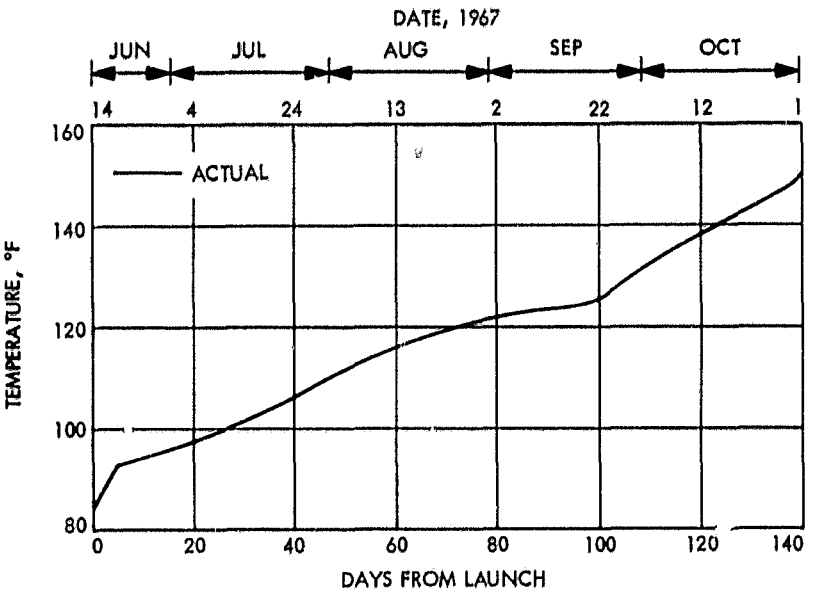

Fig. 25. Solar panel spar-zener temperature vs mission time

allowed them to dissipate nearly all of the solar array power not being used by the spacecraft. Because of the poor thermal path between the panel spars on which the diodes are mounted and the panel substrate, the power dissipated by the diodes did not contribute significantly to the substrate temperature. It was determined that the additional power drawn from the panels, coupled with the lack of substrate reheating by the zener diodes accounted for the 7°C temperature differential noted. The substrate temperature prediction was recalculated by taking the above factors into account; the data followed the new prediction closely for the remainder of the flight (Fig. 24). The actual spar temperature was plotted by using measured space simulator values for the predicted spar temperature with and without zener diode dissipation (Fig. 25).

Preliminary analysis of the I_{sc}–I_{scr} anomaly indicated that a calibration problem existed. A review of the original calibration curves and the transfer to the telemetry calibration did not reveal any discrepancies. It is theorized that the difference between the calibration resistors used on the balloon flight and those used on the *Mariner V* were the cause of the 3% higher than expected value. Further studies have failed to resolve this anomaly.

The telemetry outputs of the I_{sc}–V_{oc} transducer showed a continuous and significant degradation during the flight (see Figs. 26–28), but the solar panel performance appeared to be nominal. The ability to resolve degradation to the array is restricted, however, due to the zener diode

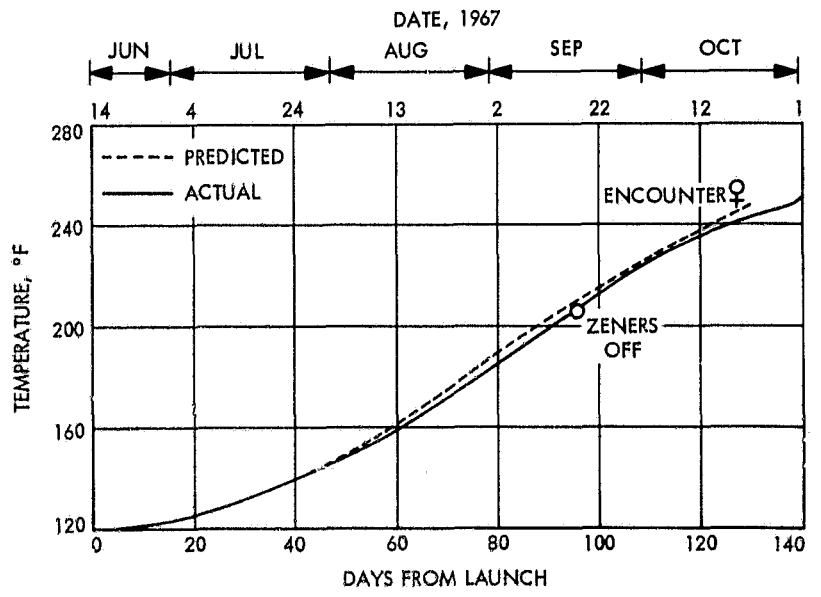

Fig. 24. Solar panel substrate temperature vs mission time

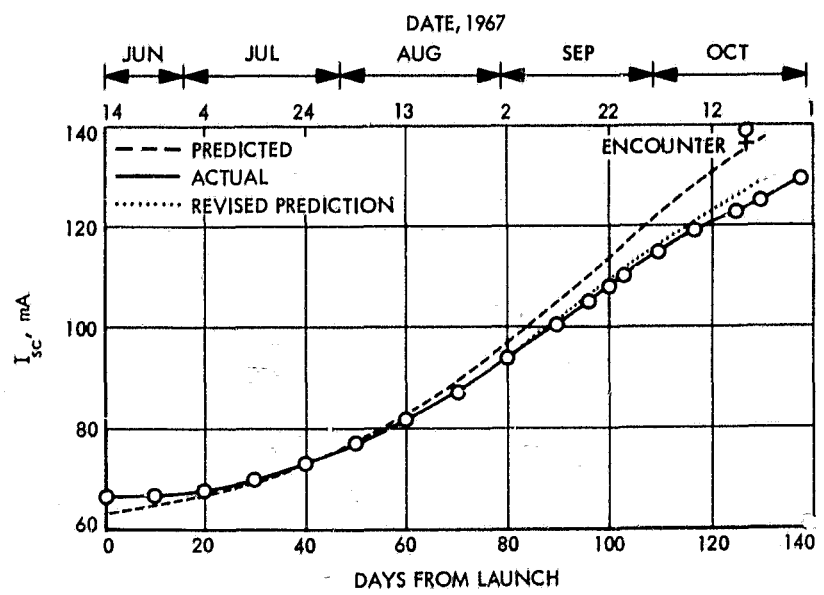

Fig. 26. Mission time vs I_{sc} cell output

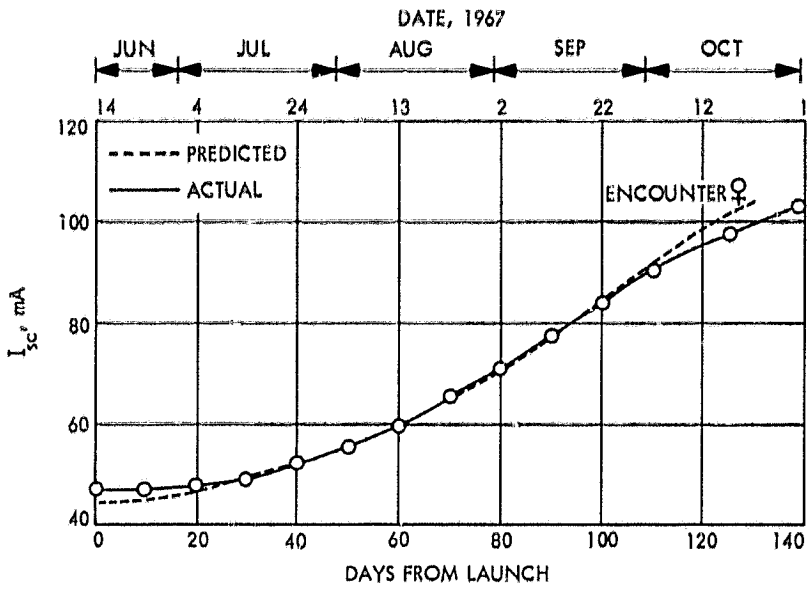

Fig. 27. Mission time vs I_{scr} cell output

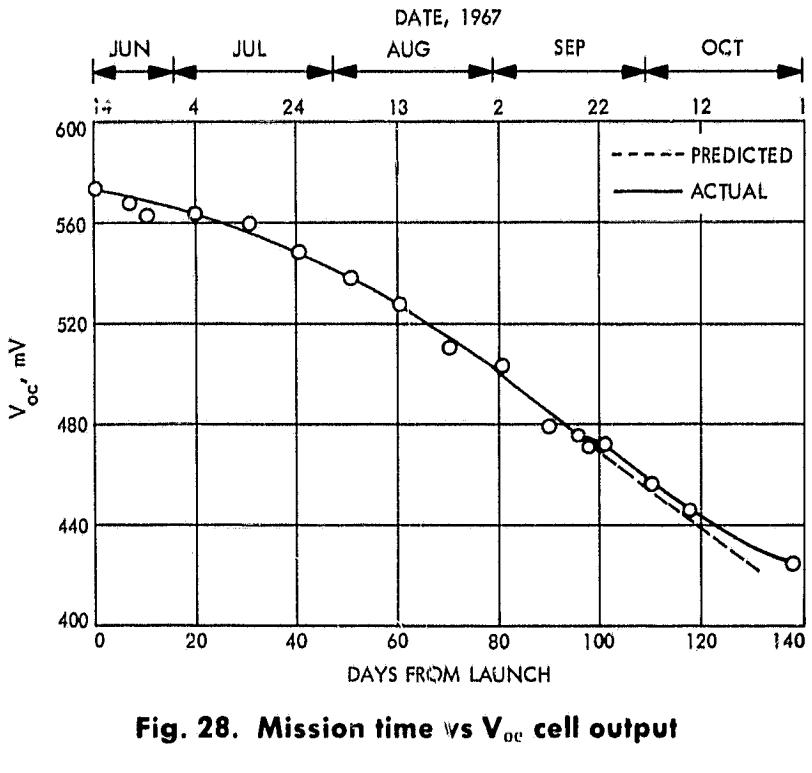

Fig. 28. Mission time vs V_{oc} cell output

limiting of the array voltage early in the flight, and operation well down on the I-V curve close to open circuit voltage later in the mission.

The rate of degradation noted in the I_{sc}–I_{scr} cells did not appear to be a function of the spacecraft heliocentric distance, nor was it the type of degradation associated with radiation damage by solar flares. A significant high-energy proton flux was not detected by the spacecraft instrumentation. Other possible sources of degradation are heat, ultraviolet radiation, and low-energy proton degradation on unprotected portions of the cells. Past studies performed at JPL have indicated that both the short-circuit current and open-circuit voltage of cells can degrade as a function of time at elevated temperature. The results of these studies did not indicate that degradation of this magnitude should be expected, however.

On the basis of the I_{sc}–V_{oc} transducer data, it must be concluded that the array had degraded by the end of mission by perhaps as much as 17%. Strict interpretation of the transducer data taken on face value indicates that approximately 10% of this degradation may be due to particle radiation, the remainder being accounted for by the other space environments, primarily heat and ultraviolet. Other interpretations of this data are possible, including load resistance changes on the transducers, low energy proton degradation on the unprotected portions of the cells, and different rates of heat degradation for irradiated and nonirradiated cells.

IV. Conditioning Equipment Modification and Test

The basis for the *Mariner* Venus 67 PCE was the *Mariner* Mars 1964 equipment. Spare *Mariner* Mars 1964 hardware was modified to perform the *Mariner* Venus 67 mission. To appreciate the design changes required, the *Mariner* Mars 1964 PCE configuration will be described, and compared with the *Mariner* Venus 67.

A. Mariner Mars 1964 Configuration

The *Mariner* Mars 1964 PCE block diagram is shown in Fig. 29. It is physically and functionally divided into two cases, Case VIII, the power regulator assembly (also called 4A8), and Case I, the power conditioning assembly. Case VIII is one large integral module; Case I consists of a frame and seven individual modules with an interconnecting harness.

The *Mariner* Mars 1964 Case VIII can be functionally divided into the power switch and logic (PS&L), two electrically identical booster regulators (B/R), a booster regulator failure sensing circuit, and battery charger control relays. The PS&L includes the following: (1) solar panel and battery logic diodes, (2) current and voltage telemetry monitors, and (3) a motor-driven switch which transfers the battery power input from a ground support power supply to the spacecraft battery. The booster regulators are identical; input power to the regulators is provided by the solar panels and/or battery in a range of 25 to 50 Vdc. The output power (a regulated 52 Vdc) supplies the inverters at loads of 27 to 150 W. The B/R provides power for cruise and encounter loads while the maneuver

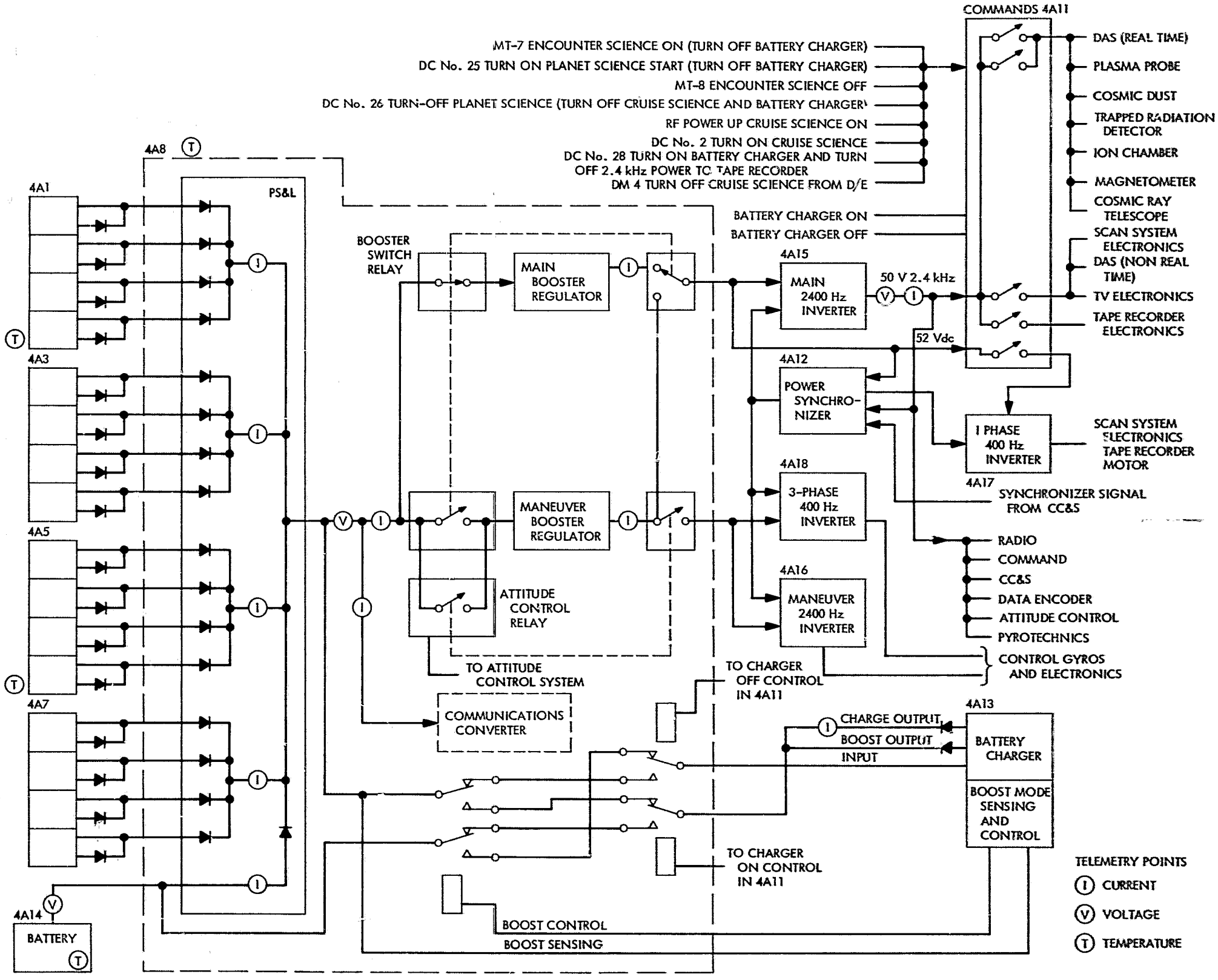

Fig. 29. Power subsystem mechanization for *Mariner* Mars 1964

B/R provides power to the maneuver loads. The maneuver B/R is also used to provide standby redundancy for the main B/R, and must, therefore, be capable of providing power to both the maneuver and main loads.

1. Case I power distribution module (4A11). This module accepts signals from the command decoder and central computer and sequencer (CC&S), and performs power switching as directed. The module uses magnetic latching relays.

2. Case I power synchronizer (4A12). The power synchronizer receives 38.4 kHz frequency reference signal from the CC&S. Internal countdown stages provide two 2.4 kHz output signals (used by the 2.4 kHz power inverters) and one 3-phase, 400-Hz output signal (used by the 400 Hz, 3-phase inverters). If the 38.4 kHz signal from the CC&S doubles in frequency or disappears, the power synchronizer will operate on its own 38.4 kHz oscillator at a reduced accuracy of 2%.

3. Case I battery charger (4A13). The battery charger performs two separate functions: battery charging and share protection. It can perform only one function at a time. Battery charging is accomplished basically by the constant potential method. Its current output is limited, however, as charging occurs in two modes: constant current and constant voltage. The share protection function is performed by a circuit called the booster (not the booster regulator). A sharing condition can occur when a transient causes the primary system voltage to equal the battery voltage. The solar panels and battery both provide current to the load (share). This condition is unnecessary if the panel power capability is equal to or slightly greater than the load required, but at some voltage higher than the battery voltage. Two conditions must be met before the booster can attempt to correct the condition. The first condition is that it be *enabled* (the charger is off), and the second condition is that the share sensor has detected a share condition from the primary system voltage (it is inhibited from detecting this condition if the spacecraft gyros are *on*). The booster then raises the primary system voltage to a point where the panels should supply all of the power. If the panel can handle the entire load, the boost circuit, after removing the share condition, will turn off automatically. If the panels cannot handle the load (power required is greater than the capability), the booster will continue to attempt to correct the share condition until commanded *off* from the ground.

4. Case I main 2.4 kHz inverter (4A15). This inverter is powered from the Case VIII main B/R regulated 52-V line. Its 2.4 kHz 50-V rms square wave is the source of the spacecraft main power. It is synchronized by the power synchronizer but is capable of free running. Its minimum efficiency at a 105-W load is 86%.

5. Case I maneuver 2.4 kHz inverter (4A16). This inverter is identical to the main 2.4 kHz inverter. Its input power is obtained from the maneuver B/R, 52-V line. The inverter powers the attitude control subsystem's maneuver electronics.

6. Case I 400-Hz single phase inverter (4A17). This inverter is powered from the main regulated 52-V line, and provides 400-Hz square wave to the scan platform motor and the tape recorder motor. It is synchronized from the power synchronizer. (This unit is not used on *Mariner* Venus 67.)

7. Case I 400-Hz three phase inverter (4A18). This inverter is a driven amplifier with signal inputs from the power synchronizer and power from the maneuver 52-V line. Its quasisquare wave output runs the gyro motors.

B. Changes From *Mariner* Mars 1964 PCE Due to Changed Power Requirements

Table 3 provides a comparison between the inputs and outputs of the *Mariner* Mars 1964 and the *Mariner* Venus 67 power subsystem. The significant changes are

Table 3. Power conditioning inputs and outputs

Inputs/outputs	*Mariner* Mars 1964	*Mariner* Venus 67
Number of diode isolated solar panel sections	16	16
Battery charger output voltage, V	34.6	34.6
Primary system voltage, V	25–50	25–50
Main 2.4 kHz output voltage, V rms	50	50
Main 2.4 kHz output power, W	50–80	50–105
Maneuver 2.4 kHz output voltage, V rms	50	50
Maneuver 2.4 kHz output power, W	5–33	5–33
400-Hz single phase inverter output voltage (No. 1), V	32.6	Not required
(No. 2), V	28.0	Not required
400-Hz three phase inverter voltage, line-to-line, V rms	27	27
400-Hz three phase inverter power total, W	10	10
Magnetometer heater power, W	Not required	3
Synchronizing signal from CC&S, kHz	38.4	38.4

as follows: (1) The main 2.4 kHz inverter (4A15) maximum output power has increased from 80 to 105 W. (2) No 400-Hz single phase power is required for *Mariner* Venus 67. (3) Raw power is required to keep the magnetometer warm.

The first requirement had the most impact on the modification of the *Mariner* Mars 1964 PCE. To maintain the 50-V output within a 2% lower tolerance, a new power transformer had to be installed in the main 2.4 kHz inverter. This transformer is bonded to the chassis and is almost impossible to remove without damaging the unit. Therefore, new main 2.4 kHz inverters were fabricated.

The increased loads on 4A15 also required changes to the power regulator (4A8). If the main B/R failed, these loads would be automatically applied to the maneuver B/R by the failure sense circuitry. These loads, in addition to the maneuver loads, would be greater than the 150-W maximum load for the B/R, as indicated in Table 4.

Table 4. B/R power loads

Unit	Maximum output power, W	Efficiency, %	Input power, W
4A15	105	86	122
4A16	33	80	41.3
4A18	10	78	12.8
4A8 telemetry monitor oscillator	NA	NA	3.6
Total max power required from maneuver B/R			179.7W

This power, 179.7 W, is 20% above the 150 W maximum for the B/Rs. The first approach considered to correct this problem was to increase the capabilities of the B/Rs. Unfortunately, the power transistors used were already being operated at the maximum desirable collector current for safe operation, and new magnetic components would have to be installed to increase B/R output power. The alternate was the addition of a circuit that would automatically remove part of the 4A15 load (the science loads) if the overload condition should occur. The conditions for an overload are: (1) main B/R fails, (2) maneuver loads are required, and (3) science loads are *on*.

Actual test and analysis showed that if the B/R input voltage is high (over 40 V) and maneuver loads are *on* only for spacecraft stability, as opposed to an actual maneuver, the load is reduced to a more acceptable 155- to 160-W range. Under these conditions, the science loads could be left *on*. Therefore, the science inhibit can be overriden by ground command (DC-V25).

Becaase 400-Hz single phase power was not required, this inverter was removed and a dummy module put in its place for structural stability in Case I.

A separately fused 0.2-A line was added to the communications converter power output to provide raw power to the magnetometer.

C. Command Logic Changes From *Mariner* Mars 1964 PCE

Except for the maneuver loads signal, all external command signals to the PCE are sent to the power distribution assembly (4A11). Circuitry inside this assembly controls magnetic latching relays to provide the correct response. The changes in command and response logic are shown in Table 5. These changes required significant modification to the power distribution module.

D. Battery Voltage Telemetry Circuit

Flight telemetry from the *Mariner* Mars 1964 indicated that the spacecraft battery continued to be charged after the flight battery charger was turned off. A current of 1.3 to 2.5 mA was flowing into the battery from the battery voltage telemetry monitor. For *Mariner* Venus 67, an amplifier with high input impedance and unity gain was added to correct the problem.

E. *Mariner* Venus 67 PCE Configuration

The *Mariner* Mars 1964 PCE, along with the above modifications, formed the basic configuration of the *Mariner* Venus 67 PCE. The overall power subsystem configuration is shown in Fig. 30.

F. Detail Design Changes to the *Mariner* Mars 1964 PCE

The changes required to modify the *Mariner* Mars 1964 to the *Mariner* Venus 67 PCE were as follows: (1) the power regulator (4A8) required the addition of several small circuits, (2) the power distribution assembly (4A11) required extensive rework of the logic, (3) the battery charger (4A13) required the addition of a sense lead to determine if it was on or off for the DCV-28 command toggling, (4) the main 2.4 kHz inverters (4A15) for *Mariner* Mars 1964 were used for spares for the *Mariner* Venus 67 maneuver 2.4 kHz inverters (4A16) and new modules were fabricated for the main inverter, (5) the maneuver

Table 5. Commands and controls

Mariner Mars 1964 commands and controls		*Mariner* Venus 67 commands and controls	
Command	**Required action by power system**	**Equivalent command**	**Required action by power system**
1. CC&S MT-7	Connect planet science to primary 2.4 kHz Connect cruise science to primary 2.4 kHz Turn on 400-Hz single phase supply Connect tape machine to primary 2.4 kHz Turn off battery charger	1. CC&S MT-7	Connect science to primary 2.4 kHz Connect tape machine to primary 2.4 kHz Turn off battery charger
2. C/D DC-V25	Same as 1, above	2. C/D DC-V25	Same as 1, above plus Will allow operation of science and maneuver attitude control if main booster regulator fails
3. CC&S MT-8	Disconnect planet science 2.4 kHz Disconnect redundant cruise science 2.4 kHz Turn off 400-Hz single phase supply	3. Not required	
4. C/D DC-V26	Same as 3, above Same as 3, above Same as 3, above Disconnect main cruise science 2.4 kHz Turn off battery charger	4. C/D DC-V26	Disconnect main science 2.4 kHz Turn-off battery charger Rescind DC-V25 override (see additional action in 2, above)
5. Spacecraft separation connector	Connect cruise science to primary 2.4 kHz Provide rf power up signal by opening normally-closed relay contact (irreversible in flight)	5. Spacecraft separation connector	Connect cruise science to primary 2.4 kHz Provide rf power up signal
6. C/D DC-V2	Connect cruise science to primary 2.4 kHz	6. C/D DC-V2	Connect science to primary 2.4 kHz Connect alternate science to primary 2.4 kHz
7. C/D DC-V28	Turn on battery charger Turn off tape electronics	7. C/D DC-V28	Turn on battery charger, or Turn off battery charger, depending on last state of charger Turn off tape electronics
8. Data encoder data mode 4	Disconnect cruise science from primary 2.4 kHz	8. Not required	

2.4 kHz inverter (4A16) was modified very slightly so that no power could be applied to it if accidently used as a main inverter, and (6) the 400-Hz single phase inverter (4A17) was removed.

G. Design Changes Required Because of *Mariner* Venus 67 Systems Testing

Two difficulties were observed in the *Mariner* Venus 67 PCE during the spacecraft testing. The first was found during radio-frequency interference (RFI) testing for the dual frequency receiver (DFR) subsystem. The DFR experiment uses two sensitive receivers at 50 MHz and 420 MHz. The booster regulators generated considerable noise at 50 MHz, which degraded the signal to noise ratio of the DFR at that frequency. Booster regulator design changes reduced the noise to an acceptable level. The second difficulty had to do with the toggling operation of the battery charger. When the battery charger turned on in the boost enable mode, it would switch itself to the charge mode rather than boost as desired. A design change to 4A11 was required to eliminate this difficulty.

1. Difficulty with 4A8 50-MHz radio frequency interference. It is not immediately obvious that the 4A8 B/Rs were capable of generating 50-MHz noise. Although the B/R is a switched mode regulator, the power transistors are slow devices and the diodes had slow reverse recovery characteristics. An investigation showed that these slow diodes did generate 50-MHz noise. The diodes during turnoff would conduct in the reverse direction for 2 to 3 μs and then turn off in about 0.1 μs. When these diodes were replaced with fast recovery diodes, there was little reverse conduction and hence no sudden changes in current as shown in Fig. 31. Much less RFI was generated, and Booster Regulator efficiency was improved slightly.

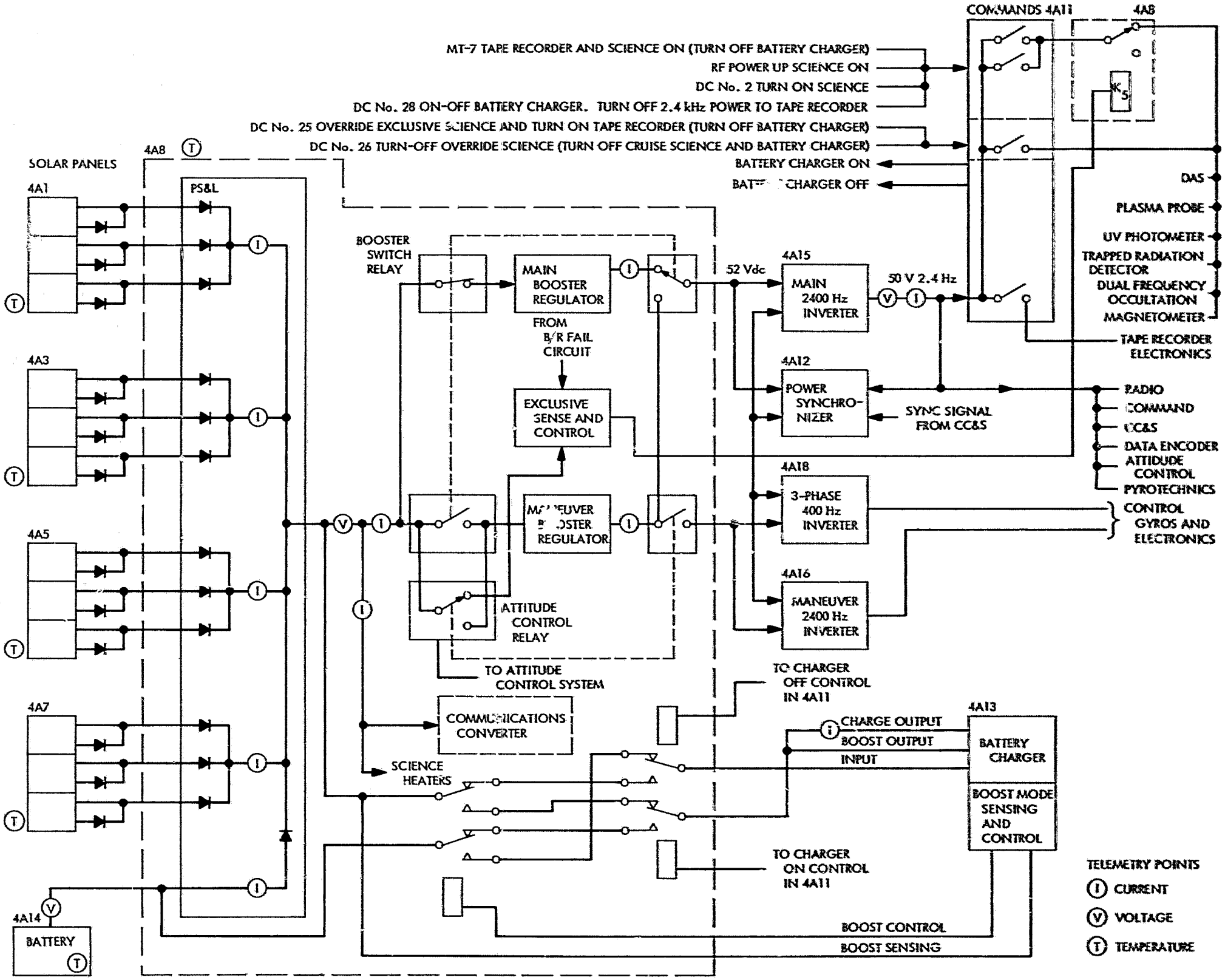

Fig. 30. *Mariner* Venus 67 power subsystem

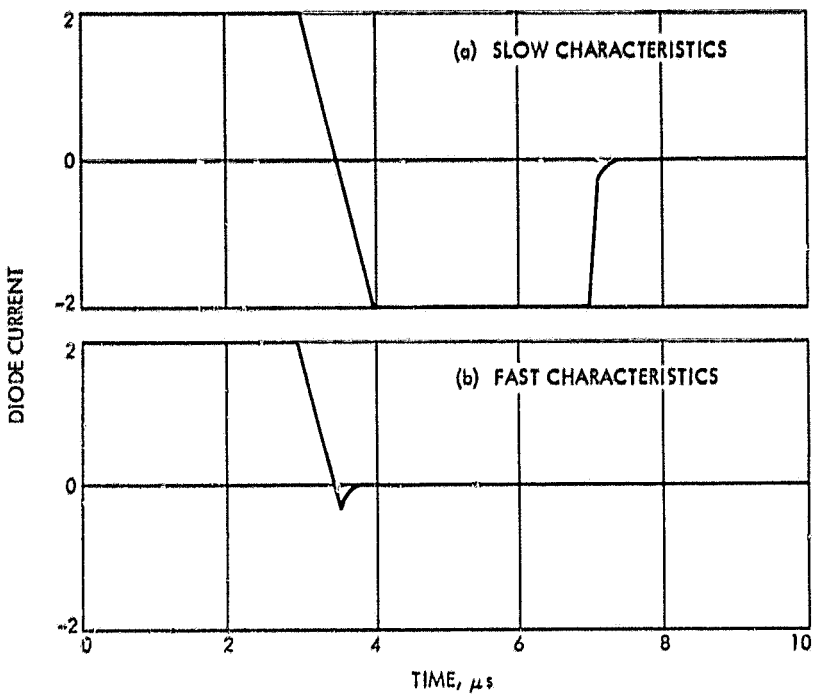

Fig. 31. Diode reverse recovery characteristics

2. ***Battery charger false switching.*** This difficulty was due to the signal to the power distribution assembly (4A11) that indicates the battery charger is *on*. When the battery charger is in boost mode, the signal is present; but, the latching relay is in the boost enable position. The signal should have prevented the relay from operating and going into charge; instead it changed the relay state. The circuit is shown in Fig. 32.

The resistors, R77 and 78, should be large enough to turn on Q30 and bleed the charge off of C13, but not so large as to transfer the relay in the process. Therefore, the resistors were changed from 56.2K to 332K each.

H. Environmental Testing

There were two spare flight qualified sets of PCE from *Mariner* Mars 1964 to be modified for the *Mariner* Venus 67 mission. There was also the *Mariner* Mars 1964 type approval set which had completed 8300 hr of life tests, as well as the *Mariner* Mars 1964 FA and the complete set of TA tests. The TA equipment required special rework to repair the 4A8 and 4A18 that had failed during the *Mariner* Mars 1964 life test.

The rework and modification of the three PCE sets was accomplished at the contractor's facility. Each module was given a thorough bench test before modification, after modification, and after complete conformal coating of the rework areas. Then, the modules of Case I were assembled and connected to the flight case harness. The assembled Case Is and the Case VIIIs (4A8) were subjected to an FA vibration test (1 min of 9.7 g rms random noise, 30–2000 Hz) in three planes. Then, an FA vacuum temperature test was performed on each assembly. This consisted of operating in a vacuum for 2 h at 0°C and 40 h at 55°C. After successful completion of the FA tests, the units were delivered to JPL. The flight units

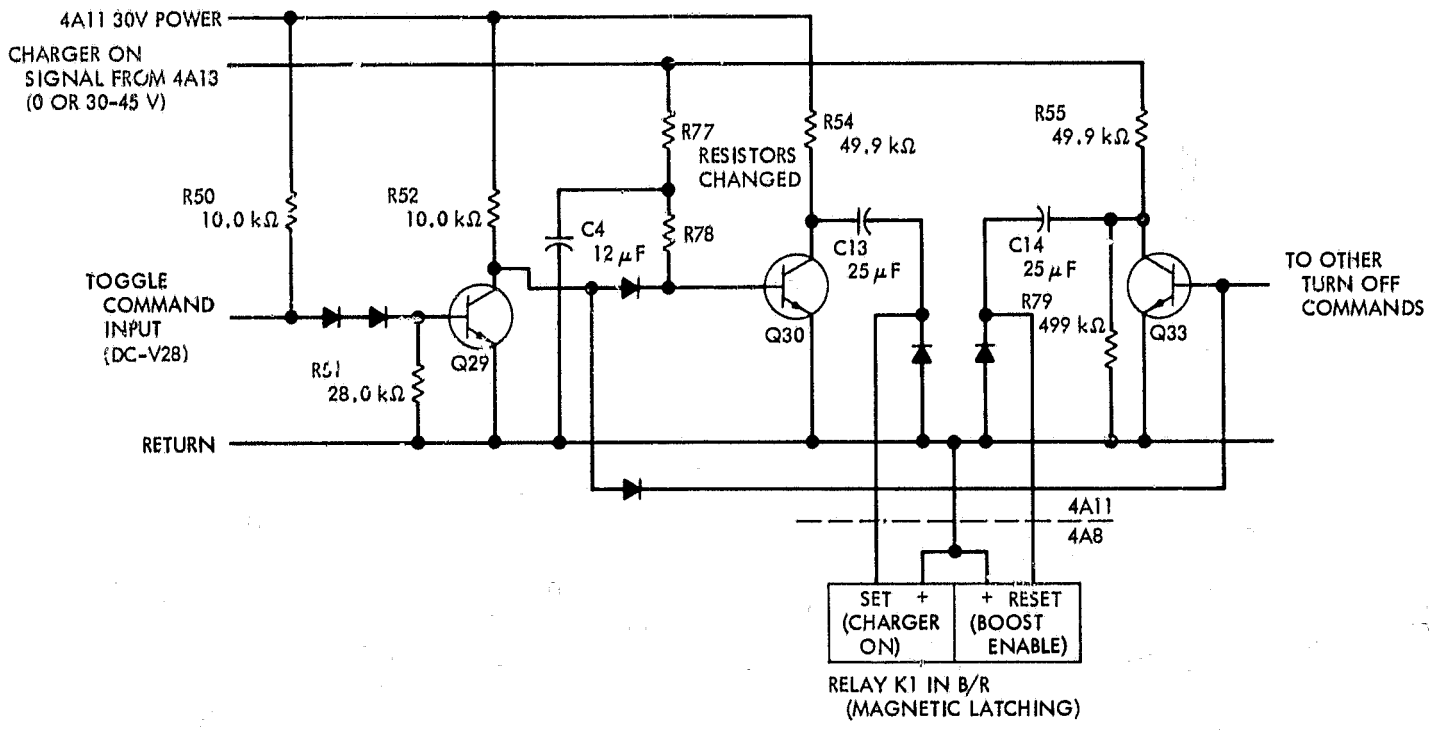

Fig. 32. Battery charger switching circuit

went into spacecraft system level testing and the TA unit into the type approval test sequence.

The TA test sequence was abbreviated because of the satisfactory TA tests on the same units for *Mariner* Mars 1964. The tests performed were: (1) TA vibration, (2) TA vacuum temperature, (3) TA shock environment, and (4) TA magnetic environment.

During the 4A8 TA vacuum temperature test, thermocouples were attached to the power transistor transducer. (The flight transducer is close to the power transistors.) When the temperature control plate attached to the 4A8 was raised to 75°C (167°F), the transistors were 132°C (270°F); the flight transducer was at 110°C (230°F). These temperatures are unrealistically high. During flight, the transducer is expected to be less than 43°C (110°F). Therefore, a waiver was granted to allow the TA vacuum temperature test to be conducted with the flight transducer at 87°C (190°F) and the transistors at 106°C (225°F). The temperature profile of the test consists of 4 h at low temperature, −10°C, and 40 h at high temperature.

I. Time Scale for Modifications

The following is the timing of the modification of *Mariner* Mars 1964 PCE and the verification of the resultant *Mariner* Venus 67 hardware:

Modification	When performed
Design and prototype modification	January 1966 to June 1966
Modification and bench testing flight and TA PCE (3 units)	June 1966 to December 1966
Flight acceptance testing	October 1966 to December 1966
Type approval testing	January 1967

J. PCE Performance During Launch and Midcourse Maneuver

The PCE on the *Mariner V* performed faultlessly through the end of the midcourse maneuver.

The main B/R operated with loads of 70 W during launch, 100 W with both gyros and science *on*, and 90 W in a cruise configuration. Efficiency of this unit during cruise was 75.5% (calculated from flight information). The flight 4A8 temperature monitor mounted close to the main B/R varied between 30°C (85°F) and 40°C (103°F).

The maneuver B/R performed well, when used during the launch phase and midcourse. Its load varied between 30 and 58.2 W. The 58.2 W was observed for short periods during the midcourse maneuver. If the main B/R was assumed to be 78% efficient at 98.3 W, then the maneuver B/R was 75% efficient. However, a 1% error (telemetry tolerance) in dual B/R input current would mean a 3% error in the maneuver B/R efficiency calculation.

The power distribution module (4A11) turned science *on* and sent an RF *power up* signal to the radio subsystem at separation; except for that, it was not exercised.

As expected, the battery charger dissipated 19 W when charging. Battery charge current was 50 mA when the battery was 34.45 V.

The main inverter load was between 51 and 83 W, the cruise load was 70.8 W, and the efficiency at a 70.8 W load was 82%.

The temperature of Case I ranged between 20°C (68°F) and 33°C (92°F).

Plots of the PS&L voltage, and the primary currents from the sources and to the power subsystem are shown in Figs. 33 and 34, respectively.

V. Battery Modification and Test

The capacity of the battery is dictated by the system energy requirements at various critical phases of the mission. Both the *Mariner* Mars 1964 and *Mariner* Venus 67 capacity requirements for the battery during launch and encounter are the same, i.e., 1200 Wh and 900 Wh, respectively. Because the system requirements are the same as the previous mission and because the battery performed well during the *Mariner* Mars 1964 mission, it was decided that basic design changes were not necessary for the *Mariner* Venus 67 batteries, other than minor improvements which would increase reliability without altering performance characteristics.

A design verification test program was conducted on battery 26 for the purpose of obtaining data to relate structural and process changes made in the current production models to any changes in battery performance and reliability, particularly at the thermal limits specified in the JPL TA specification (MVP-50623-TAT) for the *Mariner* Venus 67 batteries.

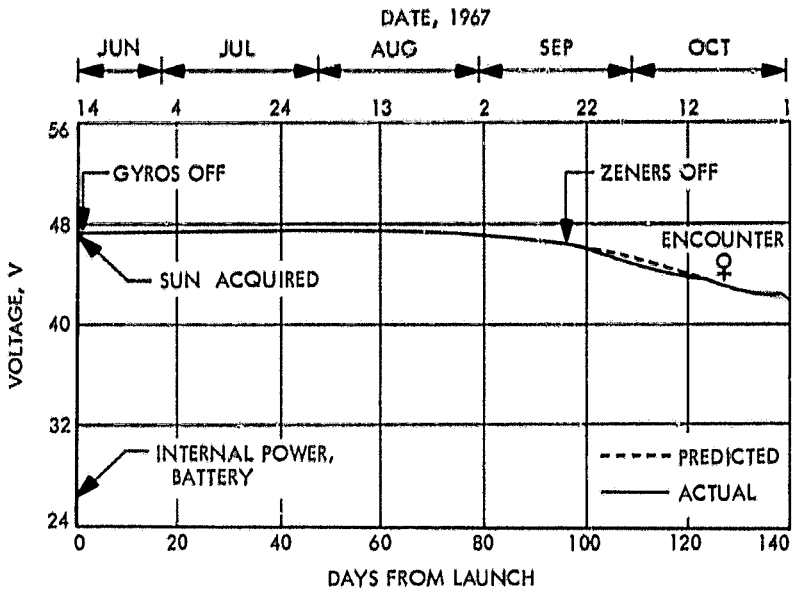

Fig. 33. PS&L voltage

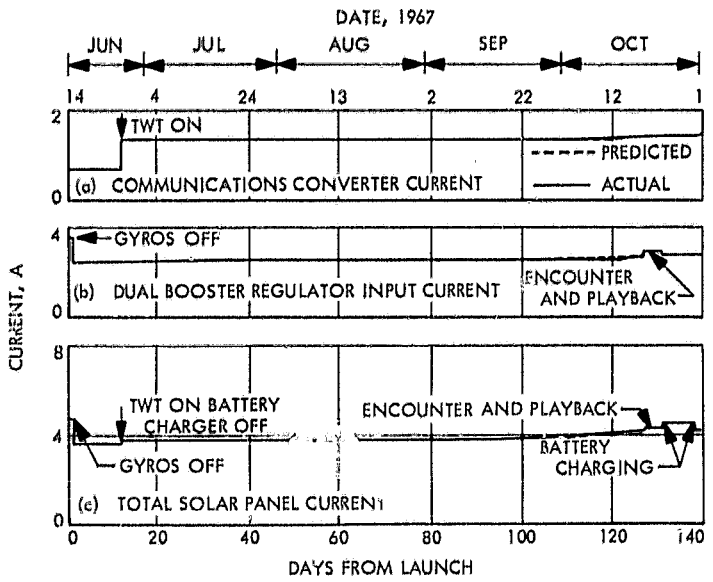

Fig. 34. Total solar panel current

The test program was specifically designed to make apparent anomalies in *Mariner* Venus 67 battery performance, due either to these changes or to other latent factors, and to verify that the batteries could meet the ampere–hour capacity requirements set forth in the TA specification. The areas of battery design specifically under consideration were: (1) the ampere–hour capacity of a *Mariner* Venus 67 battery at 32°F, (2) the ampere–hour capacity of a *Mariner* Venus 67 battery after a 5- to 10-day stand at 140°F, (3) the effects of float charging at temperatures up to 140°F, and (4) the structural integrity of the new cell cover at the type approval test level.

The changes in design and processes, described in detail later in this report, provided the *Mariner* Venus 67 batteries with improved reliability and lifetime over past production models. Life tests which were evaluated showed an increase in reliability for a period of at least the length of the proposed *Mariner* Venus 67 mission-to-planet encounter. These life tests extended the body of knowledge concerning the capabilities of the battery when their data were combined with those provided by the design verification tests.

A. Design Changes

1. Potting cover. Removing the vent tube hole of the cell cover eliminates a weak spot in the cell seal design and allows a continuous integral seal around the entire edge of the cover. Molding the cell container in Cycolac T-2502 and the cell cover and cell-lead plug in polystyrene RMD-4511 provides a cell structure of high strength.

2. Negative plate. The PVA binder for the active material has been replaced by a Teflon powder binder to improve the recombination rates of oxygen on the negative plate. No changes have been made in the ZnO or HgO contents; the active material mix provided is now 90% ZnO, 7% HgO, and 3% Teflon powder.

3. Cellophane separator. The contractor inspection processes and acceptance criteria have been changed to institute better quality control procedures on the cellophane separators. This provides a more uniform and higher quality material. The new procedure checks conductivity and pore size of the cellophane in addition to the other tests which were performed.

B. Construction Details

In Table 6, a comparison is made between the details of the *Mariner* Mars 1964 and *Mariner* Venus 67 battery construction. The only changes which appear in this table are the replacement of PVA by Teflon in the negative plate active materials, and the change in weight.

C. Discussion

1. Design and construction. The only significant change which may be directly related to performance characteristics was the replacement of PVA by Teflon powder. The replacement was intended to improve quality control. The deletion of the vent tube hole from the cell covers, and the increased quality control on the cellophane separators are more related to reliability, as is the Teflon powder, than to direct affects on discharge performance and capacity.

Table 6. Comparison of batteries

Item	*Mariner* Mars 1964	*Mariner* Venus 67
Weight, lb	33.3	33.6
Number of cells	18	18
Voltage regulation, V	25.8 to 33.48	25.8 to 33.48
Maximum safe voltage on charging, V	35.6	35.6
Float charge capability	Yes	Yes
Minimum capacity	1200 Wh launch 900 Wh encounter	1200 Wh launch 900 Wh encounter
Maximum load current, A	10	10
Maximum charging current, flight, A	1.0	1.0
Maximum charging current, GSE, A	2.0	2.0
Operating temperature, °F	30 to 140	30 to 140
Storage life at 30–50°F, minimum	1 yr	1 yr
Charge-discharge cycles, minimum	5	5
Battery isolation	Diode and fuse	Diode and fuse
Orientation of cells, spacecraft in launch position	All upright	All upright
Battery case material	Magnesium	Magnesium
Cell case material, plastic	Cycolac T-2502	Cycolac T-2502
Cells per molded unit	3	3
Cells per assembled row	9	9
Capacity loss per month at 80°F, estimated, %	2	2
Temperature transducers	1 Telemetry 1 GSE	1 Telemetry 1 GSE
Positive plates, silver		
Number per cell	12	12
Thickness, in.	0.025	0.025
Absorber	EM-312 Dynel	EM-312 Dynel
Layers of cellophane wrap	6	6
Negative plates, ZnO		
Number per cell	13	13
Thickness, in.	0.043	0.043
Retainer	Viskon 3005X	Viskon 3005X
Negative plate active materials	90% ZnO, 7% HgO, 3% PVA	90% ZnO, 7% HgO, 3% Teflon
Electrolyte concentration, KOH, %	45	45
Total plate area, $in.^2$	185	185

The average weight for *Mariner* Mars 1964 batteries, serial numbers 10 through 25 was 33.30 lb. The average weight for *Mariner* Venus 67 batteries, serial numbers 26 through 33 was 33.53 lb. This is an average weight increase of 0.23 lb/unit. The increase was brought about by a change in the assembly procedure during the battery manufacture.

The two battery row assemblies are placed into the magnesium case and then completely surrounded by potting compound. During *Mariner* Mars 1964 battery fabrication, voids sometimes occurred within the compound and in various areas within the case. An improved potting procedure on the *Mariner* Venus 67 batteries has virtually eliminated the existence of the voids, but has resulted in a greater amount of potting compound within the case. This resulted in increased battery weight over that of the *Mariner* Mars 1964 production models, and increased the mechanical strength of the assembly. This, combined with the aforementioned improvements, should enhance the reliability of the unit.

2. ***Test program.*** The test program performed on battery no. 26 provided a basis of evaluation of battery performance with respect to both the theoretical worst-case environments on the *Mariner* Venus 67 mission and the effects of certain design changes in the current production series of model 257 batteries. The test program is briefly represented by the flow diagram in Fig. 35.

The discharge of the battery at a 32°F thermal environment also indicated that a large thermal mass, maintaining a constant external temperature, can mask the actual battery capacity. This occurs when an individual cell voltage limitation, rather than a terminal voltage limitation, is used to determine discharge capacity. The cutoff voltage used was 1.43 V, terminating discharge when any cell reached this value. Figure 36, a graph of the individual cell voltages just prior to discharge termination, shows that the cells at each end of the row assemblies are the lowest in voltage with cell voltage increasing toward the center of the rows. The environmental chamber had sufficient thermal mass and cooling capacity to maintain the 32°F thermal environment against the heating effects of the battery during discharge. Because of this situation, the cells on the ends of the row assemblies were cooler than those in the center and experienced a more rapid loss of internal heat to the environment. Cell 18 was the first to reach 1.43 V, and did so after 25 A–h capacity had been removed from the battery. This is 39% beyond the requirement of the TRA specification at 32°F. However, if a battery terminal voltage of 25.8 V were used as the cutoff, an average of 1.43 V/cell, the capacity would have been considerably higher.

The next phase of the testing required a 12-day stand at 140°F in a fully charged condition, discharging the battery after 5 to 10 days at that temperature until any cell reached 1.43 V. The battery was discharged at a 10-A rate after 6 days at 140°F. The battery capacity was

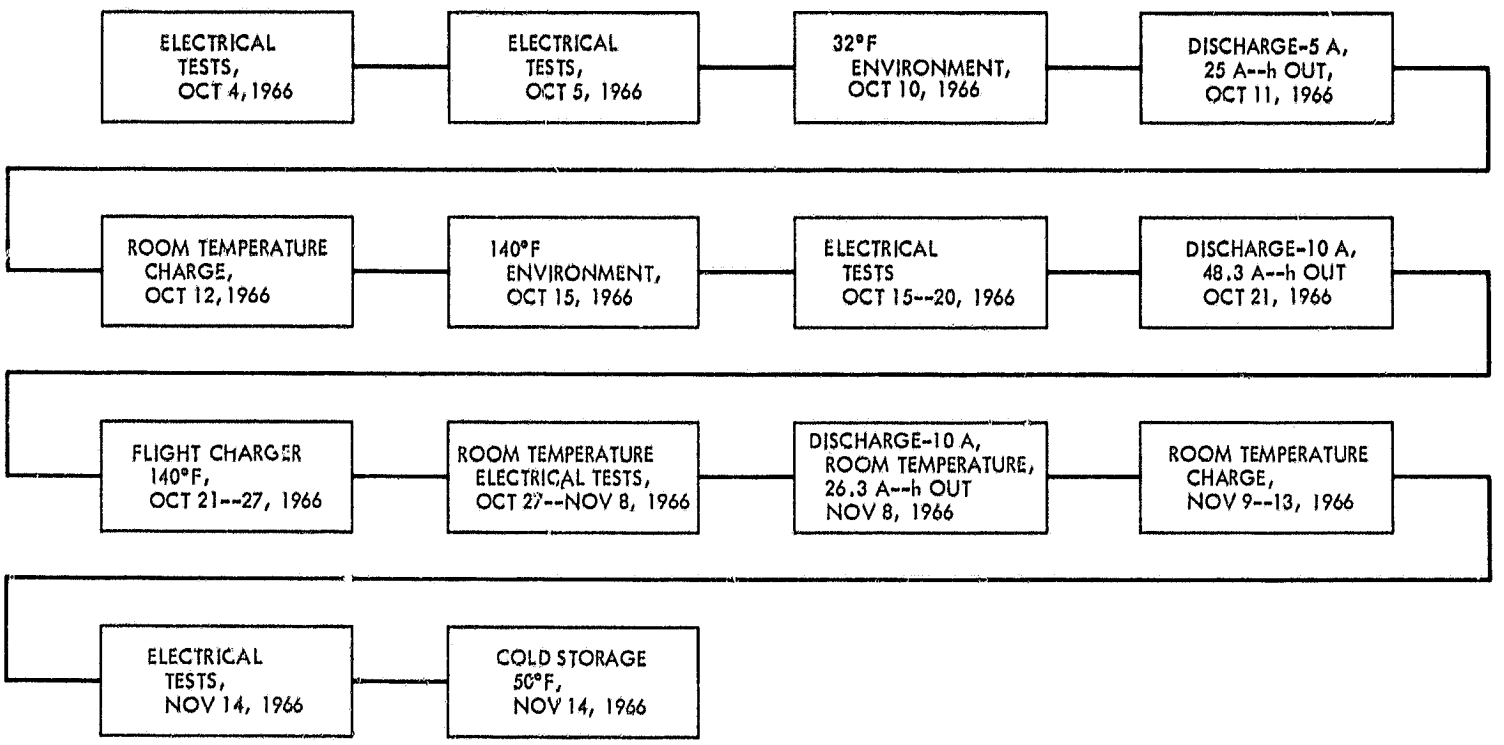

Fig. 35. Test procedure flow diagram

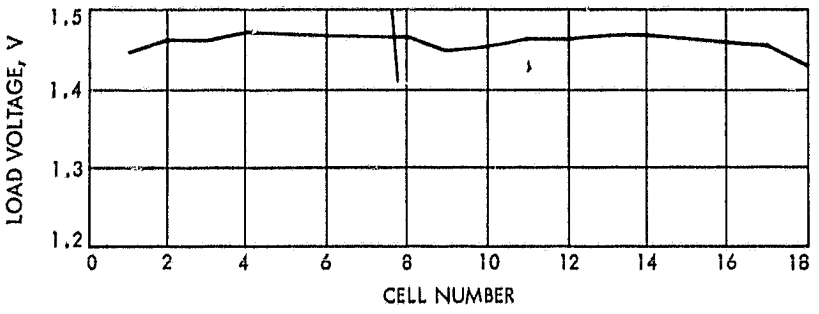

Fig. 36. Cell voltages at 32°F ambient temperature, 5-A load cutoff point, and 26.29-V terminal voltage

48.30 A–h, 101% beyond the 24 A–h requirement specified in the TA, After this discharge, the battery was charged by a flight-type charger for the duration of the 12-day period.

At that time, data indicated that cells 1, 10, and 15 were considerably lower than the remainder of the battery cells. The charger current was zero, however, indicating that the battery was fully charged. If this were true, then these cells were malfunctioning and possibly shorted. Open-circuit voltage readings were taken continuously just prior to the final capacity discharge at room temperature. Since the lowest cell had not dropped below 1.593 V, it was concluded that these cells were not shorted but that they probably had not reached full capacity in the amount of time that the battery was on the flight charger.

The battery was then discharged at room temperature at a 10-A rate with cell 15 reaching 1.43 V first. The capacity under these conditions was 26.30 A–h required by the TA specification.

After the discharge, cells 1, 10, and 15 were lower than the others with cell 15 being the limiting cell. The battery was then recharged at a terminal cutoff voltage of 35.2 V. The capacity returned indicated that the battery was not fully charged prior to the final discharge. The open-circuit voltage readings taken after the recharge showed all cells to be at or above 1.859 V. Even with the battery in a condition of partial charge, the capacity was more than that required in the TA specification. The final open-circuit voltages taken indicate that the low cells (1, 10, and 15) were in good condition and not malfunctioning. Later investigation showed that the flight charger current was still at 28 mA at the end of the 12-day period. The current readout channel on the input scanner had malfunctioned and was the cause of the zero current reading at that time.

3. ***Flight acceptance requirements.*** As one requirement of FA testing for the *Mariner* Mars 1964 batteries, one full capacity discharge at room temperature was performed on all batteries, at a 10-A rate to a 25.8 V terminal voltage. The average capacity for the batteries, serial no. 10 through 25, was 55.0 A–h. This was performed as the first cycle on the batteries. Battery 26, *Mariner* Venus 67, was discharged at room temperature, 10-A rate to 25.8 V, and

had a capacity of 53.0 A–h. This value is over 96% of that obtained from the *Mariner* Mars 1964 data, but was the fourth cycle on battery 26. It had previously undergone full capacity discharges at 32°F, 140°F, and at room temperature; batteries 10 through 25 had been discharged only once at room temperature.

D. Manufacturing and Test Results

The battery case and cell containers maintained structural integrity at all times. No cracking or electrolyte leakage were observed at any time, during, or after the test program. The battery performance under all thermal conditions surpassed the requirements of the TA specification. The final charge input and open-circuit voltages indicated that the battery was not adversely affected by either the temperature extremes or the float charging at the upper thermal limit.

The discharge curves of battery 26, typical of data obtained from the *Mariner* Venus 67 TA batteries, also showed no anomalies. Figures 37 and 38 represent the discharge curves at the two thermal extremes.

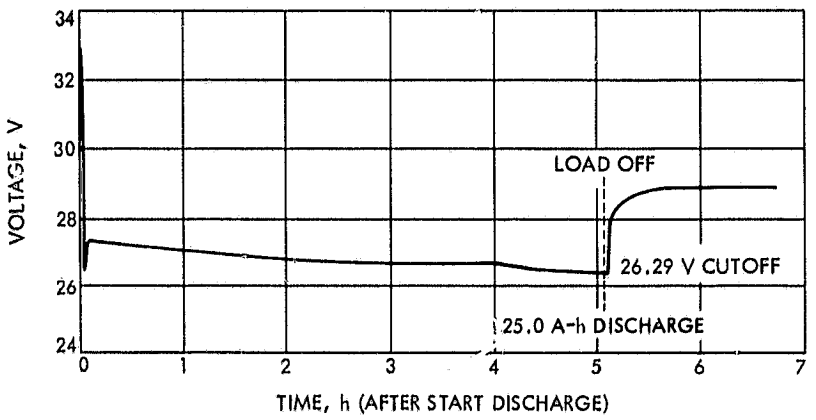

Fig. 37. Discharge curve for battery 26 at 32°F ambient temperature and 5-A discharge rate

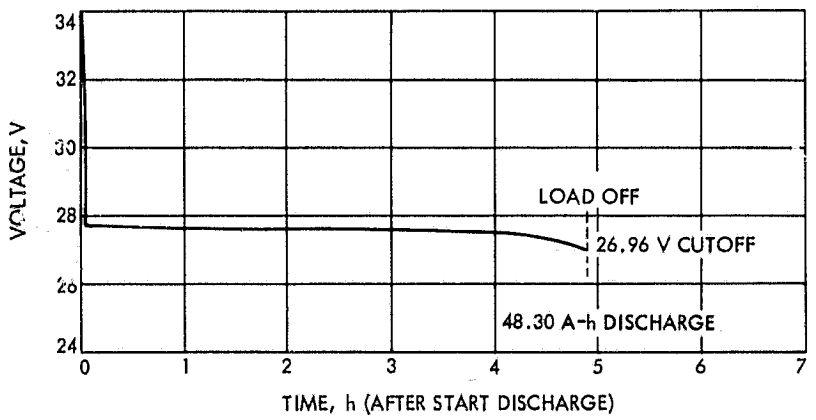

Fig. 38. Discharge curve at 140°F ambient temperature and 10-A discharge rate

The data obtained clearly indicates that the *Mariner* Venus 67 batteries are at least equal, if not better, in performance to the *Mariner* Mars 1964 batteries; batteries 6, 7, and 8 were discharged after vibration at 32°F, recharged, and discharged again at 140°F. Comparative data for discharges on these and *Mariner* Venus 67 batteries 26–29 for the design verification and TA units, are shown in Table 7.

Table 7. Battery discharge comparisons

Battery S/N		Temperature, °F	Rate	Capacity, A-h
Mariner Mars 1964	6	32°F	4A	6.0
Mariner Mars 1964	7	32°F	4A	4.0
Mariner Mars 1964	8	32°F	4A	20.0
Mariner Venus 67	26	32°F	5A	25.0
Mariner Venus 67	27	32°F	5A	23.0
Mariner Venus 67	28	32°F	5A	30.2
Mariner Venus 67	29	32°F	5A	29.0
Mariner Mars 1964	6	140°F	10A	26.0
Mariner Mars 1964	7	140°F	10A	25.0
Mariner Mars 1964	8	140°F	10A	15.0
Mariner Venus 67	26	140°F	10A	48.3
Mariner Venus 67	27	140°F	10A	28.0
Mariner Venus 67	28	140°F	10A	28.0
Mariner Venus 67	29	140°F	10A	25.0

The verification of a design is established by the physical testing of completed assemblies to specifications and requirements of some finite magnitude greater than that anticipated under normal conditions. The environmental specifications stated in the TA specification provide environmental conditions of greater severity than would be expected under normal circumstances during the mission. The data obtained from a test program meeting these requirements can, therefore, be used to predict battery design integrity and performance.

The performance analysis and evaluation derived from the design verification testing also provides a basis for approving additional production of more of the same type battery which will eventually become flight hardware. If the battery meets the performance requirements under worst-case conditions, it can then be assumed that an ample margin of design adequacy exists, and production of flight units may commence with assurance that they will be capable of functioning beyond normal flight conditions.

Since the battery operation is based on chemical reactions, it is to be expected that battery capacity is affected

by environmental temperatures. The chemical reactions between the separators, electrodes, and electrolyte that serve to degrade the capacity of the battery, decrease in activity with decreasing environmental temperatures and gas evolution; recombination decreases at the same time. This decrease in chemical activity generally eliminates damage to the internal working components of the cell. It does not eliminate the effects of differential shrinkage of the cell container materials, the potting compounds, the battery case, and possible stresses on the cell seal in the 32°F thermal environment.

The 32°F thermal environment test affects the available capacity of a battery and the structure of the cell containers and battery case. This temperature is quite useful, therefore, in evaluating the battery design and function should these conditions occur during the mission. The TA specification requires a capacity of 18 A–h at 32°F and, as previously mentioned, this battery surpassed the requirement as did all batteries on the TA test program. It may then be concluded that the design provides more than sufficient capacity in this environment. Visual observation of the battery during test, and electrical checks for shorts to the case after the tests were performed, did not indicate any evidence of electrolyte leakage nor were changes in the potting or cell structure and properties found. Insulation resistance, wiring continuity, and case isolation were all within specification and, in addition, no anomalies appeared during the capacity discharge as seen on the discharge curves. It was concluded that the *Mariner* Venus 67 battery configuration and design meet all requirements at the lower thermal environment.

The 140°F thermal environment test on a *Mariner* Venus 67 battery produces effects opposite to those described for the 32°F thermal environment. At the higher temperature, chemical activity within the battery increases and results in increasing internal discharge or capacity losses. As a part of this process, zinc on the negative plates is more soluble in the electrolyte, and silver reaction with the separators increases. The tensile strength of the epoxy used in the cell-container structural seals decreases with increasing temperature creating a higher susceptibility to electrolyte leakage.

The TA specification requires the battery to have a capacity of at least 24 A–h after a stand of 5 to 10 days at 140°F. The data from this test and from TA testing indicated that battery capacity was beyond that required. No electrolyte leakage was discovered during or after this test, no adverse effects on insulation resistance or wiring continuity were found, and no structural damage to the case or cell containers could be discerned.

The capacity of these batteries during their subjection to the 140°F thermal environment indicates that the accelerated degrading processes, at least for this relatively short period of time, are very small, and that the *Mariner* Venus 67 battery is capable of performance beyond that normally required at the elevated temperature. It may also be concluded that the structural strength of the battery case, cell containers, epoxy, and potting compound is sufficient to withstand the debilitating effects of high temperature during a deep discharge.

After being discharged at 140°F, the battery was float charged for 6 days in the same thermal environment. A number of conclusions may be drawn from the behavior of the battery during the test and supported by the data from the subsequent final discharge at room temperature. A basic effect of charging the battery, especially in a continuous mode such as this, is that gas evolution occurs within the cell. If the considerations applied to the theoretical design are valid, a recombination of the gas takes place at a sufficient rate to preclude any pressure increases beyond the strength limitations of the cell container.

One other major effect that occurs during charging is zinc dendrite growth. Under normal conditions, the negative plate retainer is of sufficient strength to provide a reasonable resistance to punctures made by the dendrites; this can create a shorting condition to the positive plates. When the battery is subjected to high temperatures, however, the subsequent heating of the electrolyte may cause the retainer material to loose its mechanical strength. This is accompanied by a consequent higher probability of cell failures due to the occurrence of shorting.

A discharge to full capacity was performed at room temperature after allowing battery 26 to stand for 11 days. The purpose was not only to allow the battery to reach internal equilibrium, but to allow any cells that may have become shorted to degrade in capacity, thus making the effect more readily discernible during the subsequent discharge.

A 26.30 A-h capacity was removed from battery no. 26 at room temperature, which was not as high as expected. No shorting was apparent in any of the cells, and it was concluded that the battery had not been fully charged due to an equipment malfunction.

A recharge sequence, initiated after the room temperature discharge, provided additional data confirming the good condition of all cells. A total of 55.5 A–h was accepted by the battery. Open-circuit voltages of all cells were excellent indicating that there was no shorting in any cell and that the active material on the plates was in excellent condition.

E. Battery Flight Operation

Spacecraft power was briefly switched from an external supply to the battery at L − 100 min and then for the final time at L − 7 min. At the time of launch the battery was capable of providing at least 54.5 A–h.

At the time of liftoff, the total amount of current the battery was supplying to the spacecraft was 5.6 A, at a voltage of 27.65 V. By L + 1 min the spacecraft load had increased to 5.8 A, and the battery terminal voltage was steady at 27.65 V. Just before sun acquisition, at L + 30 min, the battery terminal voltage was 27.5 V, with the load still at 5.8 A. This was the lowest voltage noted during launch.

The spacecraft load was removed from the battery at sun acquisition. The total capacity removed from the battery during the launch period was 4.3 A–h, assuming a nominal 55 A–h capacity prior to the L − 100 count, and adding in the capacity returned between L − 100 and L − 7 min. A total of 3.2 A–h were used between liftoff and sun acquisition.

Since the battery charger was on during the launch, the battery began to be recharged as soon as the solar panels acquired the sun. The initial charge rate was 270 mA, at 28.9 V, gradually tapering down to 30 mA, at 34.45 V, 134.05 h after the start of charge. The number of A–h replaced up to this time, at the start of the midcourse maneuver, was 4.81; the battery then had a total capacity of 55.51 A–h.

The pitch portion of the midcourse maneuver started 135.5 h after launch. As expected, when the solar panels were partially shaded by the spacecraft bus, the battery began to share with a load voltage of 27.9 V and a discharge current averaging approximately 3 A. The total sharing time was 46 min. Battery load voltage remained fairly constant, the lowest voltage being 27.8 V, which was 100 mV less than at the beginning of the pitch. The battery capacity was depleted by 2.33 A–h during the midcourse maneuver.

Figure 39 shows the battery terminal voltage profile from launch to Canopus acquisition, while Fig. 40 presents the battery charger current profile for the same period of time.

The battery charger, which had been left on since launch, again started charging at sun reacquisition. The battery was allowed to recharge until June 27, 1968: this was 13 days after launch and 7.5 days after the midcourse. The battery terminal voltage at this time was 33.45 V; an estimated 58.8 A–h capacity was available.

Within a few hours after the charger was turned off, the battery terminal voltage dropped to 33.4 V which is normal for the *Mariner* silver-zinc battery. The terminal voltage remained stable at the 33.4 V level through the remainder of the cruise, encounter, and tape playback periods.

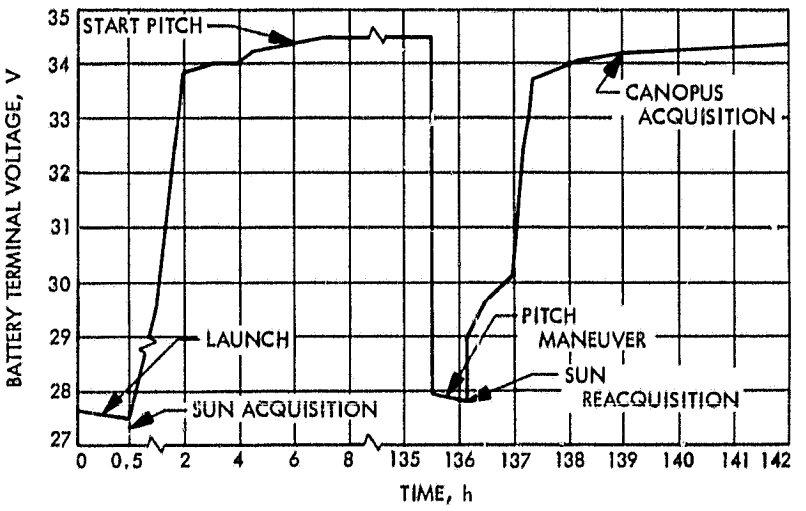

Fig. 39. Battery terminal voltage profile; launch to second Canopus acquisition

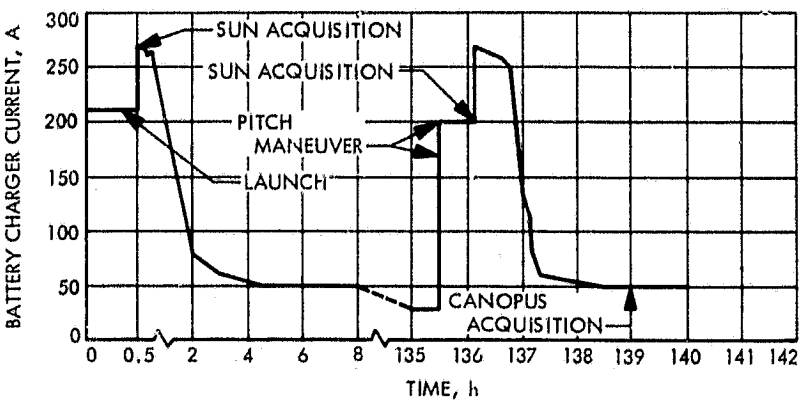

Fig. 40. Battery charger current profile; launch to second Canopus acquisition

The battery was not used again after the midcourse. However, to assist in determining the condition of the battery, the charger was turned on after the second tape playback for an additional 84 h of charging. When the charger was turned on, the terminal voltage rose to 34.45 V and the charge rate was 10 mA; this was identical to the voltage and current when the charger was turned off after the midcourse maneuver. The additional charging provided an estimated 1.2 A–h. This brought the total battery capacity to about 60.0 A–h. A curve for battery terminal voltage is shown in Fig. 41.

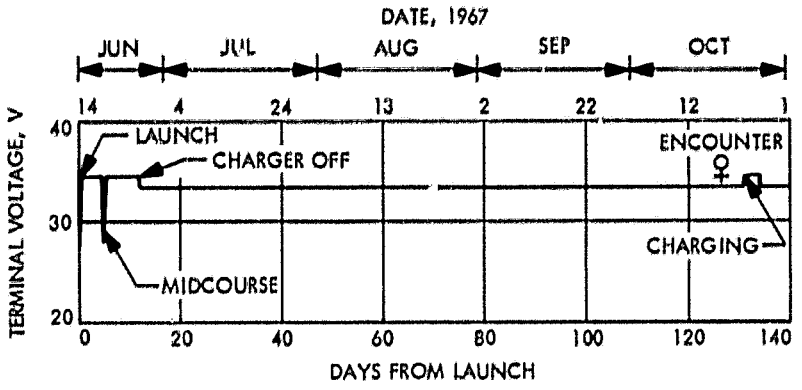

Fig. 41. Battery terminal voltage; launch to end of mission

No anomalies were noted in the battery telemetry during any of the discharge, charge, or stand periods. It is felt that the battery was in good condition when the spacecraft was prepared for the long term cruise on November 21, 1967.